SIAM J. APPLIED DYNAMICAL SYSTEMS
Vol. 10, No. 3, pp. 1100–1126

A Tangential Displacement Theory for Locating Perturbed Saddles and Their Manifolds*

Sanjeeva Balasuriya†

Abstract. The stable and unstable manifolds associated with a saddle point in two-dimensional non–area-preserving flows under general time-aperiodic perturbations are examined. An improvement to existing geometric Melnikov theory on the normal displacement of these manifolds is presented. A new theory on the previously neglected tangential displacement is developed. Together, these enable locating the perturbed invariant manifolds to leading order. An easily usable Laplace transform expression for the location of the perturbed time-dependent saddle is also obtained. The theory is illustrated with an application to the Duffing equation.

Key words. hyperbolic trajectory, nonautonomous flows, aperiodic flows, Melnikov function, saddle stagnation point, Duffing equation

AMS subject classifications. 34C45, 34E10, 34A26

DOI. 10.1137/100814640

1. Introduction.

Invariant manifolds are important entities in continuous dynamical systems, forming crucial flow organizers. Their movement under perturbations can alter the global flow structure. The original results of Melnikov [40] relate to the normal displacement of stable and unstable manifolds in a homoclinic structure in two-dimensional area-preserving flow, under a time-sinusoidal perturbation. The transverse zeroes of the so-called *Melnikov function* identify when the perturbed invariant manifolds intersect, leading to chaos via the Smale–Birkhoff theorem [26, 4, 57]. Extensions of the Melnikov method to higher dimensions [25, 44, 60, 54], time-aperiodicity and/or finite-time [41, 44, 58, 62, 8], subharmonic bifurcations [40, 57, 61, 59], nonhyperbolicity [54, 60, 63], and non–area-preservation [32] are available.

While Melnikov methods can be used to determine how invariant manifolds move *normal* to the original manifolds, there has been no method in the literature in which the tangential movement is characterized. This study addresses this issue, arriving at a Melnikov-like function for the tangential displacement, under general time-dependent perturbations. The original two-dimensional flow is assumed to contain a saddle structure but need not be area-preserving. The displacement is expressed as a function of the original position p on the manifold and the time-slice t. Along the way, a similar quantification for the normal displacement is obtained, in which potential divergence issues in the Melnikov function and the legitimacy of ignoring higher-order terms are explicitly addressed. The normal and tangential results together permit the locating of the perturbed stable and unstable manifolds of the

*Received by the editors November 11, 2010; accepted for publication (in revised form) by H. Kokubu July 9, 2011; published electronically September 20, 2011.
http://www.siam.org/journals/siads/10-3/81464.html

†School of Mathematical Sciences, University of Adelaide, Adelaide SA 5005, Australia, and Department of Mathematics, Connecticut College, New London CT 06320 (sanjeevabalasuriya@yahoo.com).

saddle point to first order in the perturbation parameter. Using a limiting procedure, the location of the "perturbed saddle point" (the hyperbolic trajectory in the augmented phase space) is also obtained, in terms of a simple expression involving Laplace transforms.

Locating perturbed stable and unstable manifolds in time-aperiodic situations has strong applicability in geophysical fluid dynamics, particularly in oceanic flows which are weakly two-dimensional [29, 46, 43, 13, 50, 39, 52, 22]. These form time-varying flow separators and specifically are the boundaries of Lagrangian coherent structures [30, 47, 28, 29, 46, 52, 20, 23]. Their determination is therefore crucial to understanding fluid transport in oceanic dynamics but remains difficult due to the fact that theoretical tools in the genuinely time-aperiodic setting are lacking. The importance of this problem is reflected by the range of ad hoc tools which have been developed to identify such flow separators: finite-time Lyapunov exponent ridges [28, 45, 52], finite-size Lyapunov exponents [35, 36], patchiness [38], ergodic partitions [42], and transfer operators [21, 22, 23]. The greatest promise of theoretically determining time-aperiodic stable and unstable manifolds may initially be in a perturbative setting—a steady flow with invariant manifolds which is then time-aperiodically perturbed. Irrespective of conventional wisdom, determining perturbed invariant manifolds does require information about both the normal and the tangential displacements, and thus the current article has significant importance in this endeavor. Furthermore, locating the "moving saddle stagnation points" to which these invariant manifolds are attached is crucial to understanding mixing processes (in the ocean, in the atmosphere, in microfluidic devices, etc.). As pointed out by Haller and Poje [29], these are not instantaneous fixed points. The results of this article enable this determination quickly using available software, since a Laplace transform expression is available. This Laplace transform technique also provides a useful tool in flow control problems in which a saddle stagnation point needs to be moved to a given location [2, 62]. An additional application to the results of this article is in determining perturbations to traveling wave profiles in reaction-diffusion systems, arising, for example, in combustion [12, 15] or mathematical biology [11, 9], since such profiles are associated exactly with perturbed heteroclinic manifolds.

This article is organized as follows. The main results, expressed in a geometrical framework, are presented in section 2. Theorems on both the normal and tangential motions of both the unstable and stable manifolds of a saddle point are provided. A theorem on the location of the new hyperbolic trajectory ("time-dependent saddle point") expressed using simple Laplace transforms is also presented. Section 3 gives the proofs of the theorems. Leaving the numerous interesting applications mentioned in the previous paragraph to the future, section 4 illustrates the theory with an application to the invariant manifolds of Duffing's equation [33, 56, 57, 37, 39, 34]. Finally, section 5 provides some concluding remarks regarding the implications of these results.

2. Results.

The system to be considered is

$$\dot{\mathbf{x}} = \mathbf{f}(\mathbf{x}) + \varepsilon\, \mathbf{g}(\mathbf{x}, t), \tag{2.1}$$

in which $\mathbf{x} \in \Omega \subset \mathbb{R}^2$, $\mathbf{f} : \Omega \to \mathbb{R}^2$, and $\mathbf{g} : \Omega \times \mathbb{R} \to \mathbb{R}^2$. The parameter ε is small: $0 < \varepsilon \ll 1$. Assume the following.

(H1) The function $\mathbf{f} \in \mathrm{C}^2(\Omega)$.

(H2) The point $\mathbf{a}$ is a saddle fixed point of (2.1) when $\varepsilon = 0$; i.e., the matrix $D\mathbf{f}$ when evaluated at $\mathbf{a}$ has real eigenvalues $\lambda_u > 0$ and $\lambda_s < 0$. The corresponding eigenvectors of $D\mathbf{f}(\mathbf{a})$ are $\mathbf{v}_u$ and $\mathbf{v}_s$, respectively.

(H3) The function $\mathbf{g}(\mathbf{x}, t)$ is in $\mathrm{C}^2(\Omega)$ for any $t \in \mathbb{R}$, and $\mathbf{g}$ and $D\mathbf{g}$ are bounded in $\Omega \times \mathbb{R}$.

The unperturbed ($\varepsilon = 0$) form of (2.1) has the phase space Ω in which it possesses a saddle fixed point $\mathbf{a}$, which has a one-dimensional unstable manifold (associated with the eigenvalue λ_u) and a one-dimensional stable manifold (associated with λ_s). These can be represented, respectively, by the trajectories $\bar{\mathbf{x}}^u(p)$ and $\bar{\mathbf{x}}^s(p)$, in which

$$\lim_{p \to -\infty} \bar{\mathbf{x}}^u(p) = \mathbf{a} = \lim_{p \to \infty} \bar{\mathbf{x}}^s(p).$$

The trajectory along the unstable direction, $\bar{\mathbf{x}}^u(p)$, is defined for $p \in (-\infty, P]$ for any P, and similarly, the trajectory along the stable direction, $\bar{\mathbf{x}}^s(p)$, is defined for $p \in [P, \infty)$ for any P. That is, no assumptions are made regarding the "other end" of each manifold, which may, for example, approach another fixed point (or even $\mathbf{a}$ again to form a homoclinic trajectory) or escape to infinity.

In the augmented phase space in which $\dot{t} = 1$ is appended to (2.1) with $\varepsilon = 0$, the saddle point $\mathbf{a}$ becomes a hyperbolic trajectory $(\mathbf{a}, t)$, with two-dimensional stable and unstable manifolds Γ^s and Γ^u, respectively. These are foliated by trajectories which are simply shifts of $\bar{\mathbf{x}}^\sigma(t)$, $\sigma = u, s$. Thus, Γ^u can be parametrized by $(p, t) \in [-\infty, P] \times \mathbb{R}$, through association with the point $(\bar{\mathbf{x}}^u(p), t)$, where p is used for "position" and t for "time." The stable manifold Γ^s is similarly parametrized using $(\bar{\mathbf{x}}^s(p), t)$.

Hyperbolicity of trajectories in nonautonomous systems is defined in terms of the variational equation along the trajectory having an exponential dichotomy property [18, p. 10], [62, Def. 2.1], [49, p. 143], [39, Def. 2.1], [44, p. 227]. The variational equation of the $\varepsilon = 0$ autonomous system in (2.1) evaluated along the trajectory $(\mathbf{a}, t)$ possesses such a dichotomy by virtue of its hyperbolicity. The projection matrix associated with the exponential dichotomy defines the local stable and unstable manifolds [39, Theorem 2.1], [62, Theorem 3.1]; indeed, the distance between trajectories lying on these manifolds and the hyperbolic trajectory decays to zero as $t \to \infty$ for the stable manifold, or as $t \to -\infty$ for the unstable manifold [64, sec. 5]. Now, set $0 < \varepsilon \ll 1$. Under the nonautonomous perturbation which remains bounded in t by hypothesis (H3), the exponential dichotomy property persists for a trajectory [62, Theorem 3.2], [64]. This is a consequence of Coppel's "roughness theorem" on the persistence of exponential dichotomies under bounded perturbations [18, p. 34] (specific bounds on this are obtainable [53, Theorem 2.1], but for our purposes it suffices to know that this works for sufficiently small ε). The implication is that there exists a trajectory $\mathbf{a}_\varepsilon(t)$ which is $\mathcal{O}(\varepsilon)$-close to $\mathbf{a}$ for $t \in \mathbb{R}$, such that it inherits perturbed versions Γ^u_ε and Γ^s_ε of the stable and unstable manifolds, which are $\mathcal{O}(\varepsilon)$-close to Γ^u and Γ^s, respectively, in appropriate (p, t)-domains (this is a special case of Yi's main theorem [64, p. 279]). (There are also similar versions of manifold persistence requiring different hypotheses to those used here [44, 31, 19].) It must be emphasized that $\mathbf{a}_\varepsilon(t)$ is not necessarily an instantaneous fixed point of (2.1) (that is, it cannot be obtained by setting the right-hand side equal to zero at each fixed t); a detailed analysis of the relationship between instantaneous saddle points and a corresponding hyperbolic entity for the area-preserving instance is available [29].

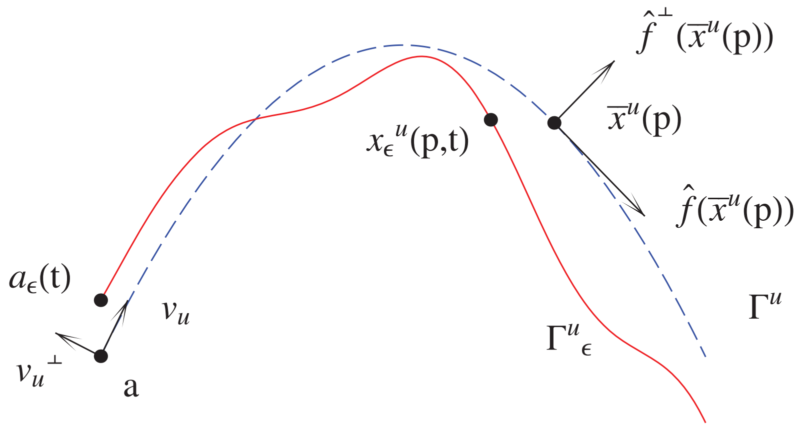

Figure 1. *Relevant part of unstable manifold structure in a time-slice t. The components of the vector $\mathbf{x}^u_\varepsilon(p,t) - \bar{\mathbf{x}}^u(p)$ normal and tangential to Γ^u are characterized in Theorems 2.1 and 2.3.*

To find the perturbation of Γ^u, fix $(p,t) \in [-\infty, P] \times (-\infty, T]$. In other words, consider a fixed time-slice t and a point $\bar{\mathbf{x}}^u(p)$. Figure 1 shows these entities in the time-slice t, and the intersection of Γ^u with the time-slice is displayed with a dashed curve, whereas that of Γ^u_ε is solid. Now, there is a trajectory $(\mathbf{x}^u_\varepsilon(p,\tau),\tau)$ on Γ^u_ε such that the point $\mathbf{x}^u_\varepsilon(p,t)$ is $\mathcal{O}(\varepsilon)$-close to $\bar{\mathbf{x}}^u(p)$ for $\tau \in [-\infty, T]$. Define the "perpendicular vector" for vectors in $\Omega \subset \mathbb{R}^2$ (obtained by rotating a vector by $+\pi/2$ in Ω) by

$$\mathbf{F}^{\perp}(\mathbf{x}) = J\,\mathbf{F}(\mathbf{x})\,, \tag{2.2}$$

in which

$$J := \begin{pmatrix} 0 & -1 \\ 1 & 0 \end{pmatrix} \quad \text{and} \quad J^T = J^{-1} = \begin{pmatrix} 0 & 1 \\ -1 & 0 \end{pmatrix} = -J, \tag{2.3}$$

and thus $\mathbf{F} = J^T \mathbf{F}^{\perp}$. Next, define the (scalar) "wedge product" by

$$\mathbf{F} \wedge \mathbf{G} := \mathbf{F}^{\perp} \cdot \mathbf{G} = \mathbf{G}^T J\,\mathbf{F} = \mathbf{F}^T J^T\,\mathbf{G}. \tag{2.4}$$

Now, in the time-slice t, the distance from $\mathbf{x}^u_\varepsilon(p,t)$ to $\bar{\mathbf{x}}^u(p)$, measured perpendicular to the original manifold, can be represented by

$$d^u(p,t,\varepsilon) := \hat{\mathbf{f}}^{\perp}(\bar{\mathbf{x}}^u(p)) \cdot \left[\mathbf{x}^u_\varepsilon(p,t) - \bar{\mathbf{x}}^u(p)\right], \tag{2.5}$$

in which $\hat{\mathbf{f}}^{\perp}$ is the unit vector in the direction of $\mathbf{f}^{\perp}$.

Theorem 2.1 (unstable manifold's normal displacement). *The quantity $d^u(p,t,\varepsilon)$ can be expanded in ε in the form*

$$d^u(p,t,\varepsilon) = \varepsilon\,\frac{M^u(p,t)}{|\mathbf{f}(\bar{\mathbf{x}}^u(p))|} + \mathcal{O}(\varepsilon^2), \tag{2.6}$$

in which the unstable Melnikov function is the convergent improper integral

$$M^u(p,t) = \int_{-\infty}^{p} \exp\left[\int_{\tau}^{p} \nabla\cdot\mathbf{f}(\bar{\mathbf{x}}^u(\xi))\,\mathrm{d}\xi\right] \mathbf{f}(\bar{\mathbf{x}}^u(\tau)) \wedge \mathbf{g}(\bar{\mathbf{x}}^u(\tau), \tau+t-p)\,\mathrm{d}\tau. \tag{2.7}$$

Proof. See section 3.1. ■

Remark 2.2. If the parametrization is reinterpreted, (2.7) is of the familiar Melnikov form [40, 26, 4, 57] in which *distances* between stable and unstable manifolds in *area-preserving* (incompressible, divergence-free, Hamiltonian) $\mathbf{f}$ are considered. The non–area-preserving adjustment is based on the development by Holmes [32] and is presented in detail in the proof.

Next, the displacement of Γ_ε^u in the direction tangential to the original manifold is sought. Referring to Figure 1, for a particular value of p (say, p_1), a perpendicular at $\bar{\mathbf{x}}^u(p_1)$, in the direction of $\mathbf{f}^\perp\left(\bar{x}^u(p_1)\right)$ would intersect Γ_ε^u at one point. Hence, one might imagine that there is *no* tangential movement at any p_1. However, the above situation corresponds to the point $\mathbf{x}_\varepsilon^u(p_1,t)$ being exactly in the direction $\mathbf{f}^\perp$ from the point $\bar{\mathbf{x}}^u(p_1)$. If a different p value is chosen, such as the one in Figure 1, a nontrivial displacement in the tangential direction would generically occur. Hence, using only the normal displacement to locate the perturbed manifold in the situation pictured in Figure 1 at the point $\bar{\mathbf{x}}(p)$ would result in the perturbed manifold being located *closer* to Γ^u than it really is.

The above problem arises from the fact that the trajectory $\mathbf{x}_\varepsilon^u$ defined in (3.1) is not unique, since there will be a collection of nearby trajectories on Γ_ε^u which satisfy this condition. A particular trajectory needs to be picked before tangential displacements from this "reference trajectory" can be discussed. This issue does not arise if focusing only on the normal displacement of the manifolds. To proceed, the idea is to choose $\mathbf{x}_\varepsilon^u$ to be the one which lies exactly on the normal to the manifold drawn at $\bar{\mathbf{x}}^u(0)$ for each and every choice of (p,t). Since $\bar{\mathbf{x}}^u(0)$ is $\mathcal{O}(\varepsilon)$-close to $\mathbf{x}_\varepsilon^u(p,t-p)$, the appropriate time-slice to represent this closeness is $t-p$. Hence, this amounts to imposing the condition

$$\mathbf{f}\left(\bar{\mathbf{x}}^u(0)\right)\cdot\left[\mathbf{x}_\varepsilon^u(p,t-p)-\bar{\mathbf{x}}^u(0)\right]=0. \tag{2.8}$$

Now, the tangential displacement at a general (p,t) is

$$c^u(p,t,\varepsilon):=\hat{\mathbf{f}}\left(\bar{\mathbf{x}}^u(p)\right)\cdot\left[\mathbf{x}_\varepsilon^u(p,t)-\bar{\mathbf{x}}^u(p)\right], \tag{2.9}$$

in which $\hat{\mathbf{f}}$ is the unit vector in the direction of $\mathbf{f}$. Define the function

$$\begin{aligned}\Omega^u(\xi) &:= \frac{\mathbf{f}^T\left(\bar{\mathbf{x}}^u(\xi)\right)\left[(D\mathbf{f})^T\left(\bar{\mathbf{x}}^u(\xi)\right)+D\mathbf{f}\left(\bar{\mathbf{x}}^u(\xi)\right)\right]\mathbf{f}^\perp\left(\bar{\mathbf{x}}^u(\xi)\right)}{\left|\mathbf{f}\left(\bar{\mathbf{x}}^u(\xi)\right)\right|^2}\\ &= \hat{\mathbf{f}}^T\left(\bar{\mathbf{x}}^u(\xi)\right)\left[(D\mathbf{f})^T\left(\bar{\mathbf{x}}^u(\xi)\right)+D\mathbf{f}\left(\bar{\mathbf{x}}^u(\xi)\right)\right]\hat{\mathbf{f}}^\perp\left(\bar{\mathbf{x}}^u(\xi)\right).\end{aligned} \tag{2.10}$$

Borrowing terminology from fluid mechanics in which $S=D\mathbf{f}+(D\mathbf{f})^T$ represents the symmetric "rate of strain tensor" [27], Ω^u shall be called the projected rate of strain. Notice that it can also be written as $\hat{\mathbf{f}}^T(-JS)\,\hat{\mathbf{f}}$, in which the $-\pi/2$-rotated rate of strain tensor yields a quadratic form in $\hat{\mathbf{f}}$.

Theorem 2.3 (unstable manifold's tangential displacement). *The quantity $c^u(p,t,\varepsilon)$ can be expanded in ε in the form*

$$c^u(p,t,\varepsilon)=\varepsilon\,\frac{B^u(p,t)}{\left|\mathbf{f}\left(\bar{\mathbf{x}}^u(p)\right)\right|}+\mathcal{O}(\varepsilon^2), \tag{2.11}$$

in which

$$B^u(p,t) = |\mathbf{f}(\bar{\mathbf{x}}^u(p))|^2 \int_0^p \frac{\Omega^u(\tau) M^u(p,\tau{+}t{-}p) + \mathbf{f}(\bar{\mathbf{x}}^u(\tau)\cdot \mathbf{g}(\bar{\mathbf{x}}^u(\tau),\tau{+}t{-}p)}{|\mathbf{f}(\bar{\mathbf{x}}^u(\tau))|^2} \mathrm{d}\tau. \tag{2.12}$$

Proof. See section 3.2. ∎

Remark 2.4. Unlike for the normal displacement, no nice simplifications occur in the case of area-preserving (incompressible) flows in which $\mathrm{Tr}\, D\mathbf{f} = \nabla \cdot \mathbf{f} = 0$. Irrotational (potential) flows in which $\nabla \wedge \mathbf{f} = 0$ also offer no simplifications to (2.12).

Remark 2.5. The term $\mathbf{f} \cdot \mathbf{g}$ in the integrand is as expected; however, an additional complicated expression involving the rate of strain tensor and the unstable Melnikov function also appears. Thus, M^u needs to have been computed before evaluating the tangential movement of the manifold.

Remark 2.6. In view of Theorems 2.1 and 2.3, the $\mathcal{O}(\varepsilon)$ movement of Γ^u_ε in relation to Γ^u can be expressed as follows. A parametrization of Γ^u can be defined in terms of (p,t) through association with the point $(\bar{\mathbf{x}}^u(p), t)$, which perturbs to $(\mathbf{x}^u_\varepsilon(p,t), t)$, which lies on Γ^u_ε. This movement can be represented by

$$\begin{aligned} \mathbf{x}^u_\varepsilon(p,t) &= \bar{\mathbf{x}}^u(p) + \left[d^u(p,t,\varepsilon)\hat{\mathbf{f}}^\perp(\bar{\mathbf{x}}^u(p)) + c^u(p,t,\varepsilon)\hat{\mathbf{f}}(\bar{\mathbf{x}}^u(p)) \right] \\ &= \bar{\mathbf{x}}^u(p) + \varepsilon \left[\frac{M^u(p,t)}{|\mathbf{f}(\bar{\mathbf{x}}^u(p))|} \hat{\mathbf{f}}^\perp(\bar{\mathbf{x}}^u(p)) + \frac{B^u(p,t)}{|\mathbf{f}(\bar{\mathbf{x}}^u(p))|} \hat{\mathbf{f}}(\bar{\mathbf{x}}^u(p)) \right] + \mathcal{O}(\varepsilon^2). \end{aligned} \tag{2.13}$$

Next, a similar determination of the normal and tangential motion of the stable manifold of $\mathbf{a}$ is obtained. The unperturbed system possessed a stable manifold representable as the trajectory $\bar{\mathbf{x}}^s(p)$ for $p \in [P,\infty)$ for any finite P (information on the beginning of the manifold is not needed). This trajectory approaches $\mathbf{a}$ along the direction $\mathbf{v}^s$, with exponential decay rate λ_s, as $p \to \infty$. In the appended phase space, the hyperbolic trajectory $(\mathbf{a},\tau)$ possesses a two-dimensional stable manifold Γ^s, parametrized by $(p,\tau) \in [P,\infty) \times [T,\infty)$ for any finite P and T. Consider now a fixed time-slice t, and consider the solution $\mathbf{x}^s_\varepsilon(p,\tau)$ which is $\mathcal{O}(\varepsilon)$-close to $\bar{\mathbf{x}}(\tau - t + p)$ for $\tau \in [T,\infty]$. As for the unstable manifold, choose the tangential reference location to satisfy

$$\mathbf{f}^\perp(\bar{\mathbf{x}}^s(0)) \wedge [\mathbf{x}^s_\varepsilon(p, t-p) - \bar{\mathbf{x}}^s(0)] = 0, \tag{2.14}$$

representing the choice of $\mathbf{x}^s_\varepsilon$ which lies in the normal direction to Γ^s at $\bar{\mathbf{x}}^s(0)$ in the time-slice $t-p$. Let the perpendicular displacement of Γ^s, in the time-slice t, at the location $\bar{\mathbf{x}}^s(p)$ be given by

$$d^s(p,t,\varepsilon) := \hat{\mathbf{f}}^\perp(\bar{\mathbf{x}}^s(p)) \cdot [\mathbf{x}^s_\varepsilon(p,t) - \bar{\mathbf{x}}^s(p)]\,. \tag{2.15}$$

This situation can be visualized by reversing all the vectors in Figure 1.

Theorem 2.7 (stable manifold's normal displacement). *The quantity $d^s(p,t,\varepsilon)$ can be expanded in ε in the form*

$$d^s(p,t,\varepsilon) = \varepsilon \frac{M^s(p,t)}{|\mathbf{f}(\bar{\mathbf{x}}^s(p))|} + \mathcal{O}(\varepsilon^2), \tag{2.16}$$

in which the stable Melnikov function is the convergent improper integral

$$M^s(p,t) = -\int_p^\infty \exp\left[\int_\tau^p \nabla\cdot\mathbf{f}\left(\bar{\mathbf{x}}^s(\xi)\right)\mathrm{d}\xi\right]\mathbf{f}\left(\bar{\mathbf{x}}^s(\tau)\right)\wedge\mathbf{g}\left(\bar{\mathbf{x}}^s(\tau),\tau+t-p\right)\mathrm{d}\tau. \tag{2.17}$$

Proof. See section 3.3. ■

Analogously to the unstable manifold, define the tangential displacement by

$$c^s(p,t,\varepsilon) := \hat{\mathbf{f}}\left(\bar{\mathbf{x}}^s(p)\right)\cdot\left[\mathbf{x}_\varepsilon^s(p,t) - \bar{\mathbf{x}}^s(p)\right] \tag{2.18}$$

and the projected rate of strain tensor function by

$$\Omega^s(\xi) := \hat{\mathbf{f}}^T\left(\bar{\mathbf{x}}^s(\xi)\right)\left[(D\mathbf{f})^T\left(\bar{\mathbf{x}}^s(\xi)\right) + D\mathbf{f}\left(\bar{\mathbf{x}}^s(\xi)\right)\right]\hat{\mathbf{f}}^\perp\left(\bar{\mathbf{x}}^s(\xi)\right). \tag{2.19}$$

Theorem 2.8 (stable manifold's tangential displacement). *The quantity $c^s(p,t,\varepsilon)$ can be expanded in ε in the form*

$$c^s(p,t,\varepsilon) = \varepsilon\,\frac{B^s(p,t)}{\left|\mathbf{f}\left(\bar{\mathbf{x}}^s(p)\right)\right|} + \mathcal{O}(\varepsilon^2), \tag{2.20}$$

in which

$$B^s(p,t) = \left|\mathbf{f}\left(\bar{\mathbf{x}}^s(p)\right)\right|^2\int_0^p \frac{\Omega^s(\tau)M^s(p,\tau+t-p) + \mathbf{f}\left(\bar{\mathbf{x}}^s(\tau)\right)\cdot\mathbf{g}\left(\bar{\mathbf{x}}^s(\tau),\tau+t-p\right)}{\left|\mathbf{f}\left(\bar{\mathbf{x}}^s(\tau)\right)\right|^2}\mathrm{d}\tau. \tag{2.21}$$

Proof. See section 3.4. ■

Remark 2.9. Since Γ_ε^s can be parametrized by (p,t) by associating with the point $\mathbf{x}_\varepsilon^s(p,t)$, the perturbed manifold is located according to

$$\mathbf{x}_\varepsilon^s(p,t) = \bar{\mathbf{x}}^s(p) + \varepsilon\left[\frac{M^s(p,t)}{\left|\mathbf{f}\left(\bar{\mathbf{x}}^s(p)\right)\right|}\hat{\mathbf{f}}^\perp\left(\bar{\mathbf{x}}^s(p)\right) + \frac{B^s(p,t)}{\left|\mathbf{f}\left(\bar{\mathbf{x}}^s(p)\right)\right|}\hat{\mathbf{f}}\left(\bar{\mathbf{x}}^s(p)\right)\right] + \mathcal{O}(\varepsilon^2). \tag{2.22}$$

The location of the perturbed hyperbolic trajectory $\mathbf{a}_\varepsilon(t)$ with respect to $\mathbf{a}$ can be determined from the above results. Suppose the eigenvectors at $\mathbf{a}$ are chosen to be in the direction of flow; that is, $\mathbf{v}_u$ points out of $\mathbf{a}$ while $\mathbf{v}_s$ points in to $\mathbf{a}$. See Figure 2. Let $\hat{\mathbf{v}}_u$ be the unit vector in the direction of $\mathbf{v}_u$, $\hat{\mathbf{v}}_u^\perp$ the unit vector in the direction of $\mathbf{v}_u^\perp = J\mathbf{v}_u$, and similarly for $\hat{\mathbf{v}}_s$ and $\hat{\mathbf{v}}_s^\perp$. Define the standard Laplace transform for τ-dependent functions h by

$$\mathcal{L}_\tau\left\{h(\tau)\right\}(s) := \int_0^\infty h(\tau)\,e^{-s\tau}\,\mathrm{d}\tau.$$

Then, by "going back" along the manifolds Γ_ε^u and Γ_ε^s toward $\mathbf{a}$, the following is obtainable.

Theorem 2.10 (perturbed saddle trajectory). *The perturbation of $\mathbf{a}_\varepsilon(t)$ from $\mathbf{a}$ can be represented through projections to the directions $\hat{\mathbf{v}}_u^\perp$ and $\hat{\mathbf{v}}_s^\perp$ by*

$$\left.\begin{aligned}\left(\mathbf{a}_\varepsilon(t)-\mathbf{a}\right)\cdot\hat{\mathbf{v}}_u^\perp &= \varepsilon\,\alpha_u(t) + \mathcal{O}\left(\varepsilon^2\right)\\ \left(\mathbf{a}_\varepsilon(t)-\mathbf{a}\right)\cdot\hat{\mathbf{v}}_s^\perp &= \varepsilon\,\alpha_s(t) + \mathcal{O}\left(\varepsilon^2\right)\end{aligned}\right\}, \tag{2.23}$$

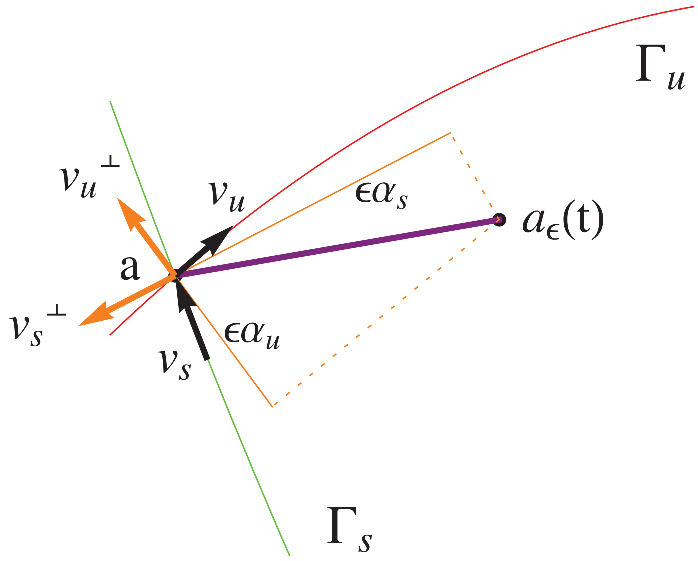

Figure 2. *Locating the perturbed hyperbolic trajectory in a time-slice t. The components of the vector $\mathbf{a}_\varepsilon(t) - \mathbf{a}$ in the directions $\mathbf{v}_u^\perp$ and $\mathbf{v}_s^\perp$, α_u and α_s, are characterized in Theorem 2.10.*

in which the leading-order displacements are

$$\left.\begin{array}{l} \alpha_u(t) := \mathcal{L}_\tau \left\{ \mathbf{g}\left(\mathbf{a}, t-\tau\right) \cdot \hat{\mathbf{v}}_u^\perp \right\} (-\lambda_s) \\ \alpha_s(t) := -\mathcal{L}_\tau \left\{ \mathbf{g}\left(\mathbf{a}, t+\tau\right) \cdot \hat{\mathbf{v}}_s^\perp \right\} (\lambda_u) \end{array}\right\} . \tag{2.24}$$

Hence, $\mathbf{a}_\varepsilon(t)$'s location can be described in the orthogonal system of unit vectors $(\hat{\mathbf{v}}_u, \hat{\mathbf{v}}_u^\perp)$ by

$$\mathbf{a}_\varepsilon(t) = \mathbf{a} + \varepsilon \left[\alpha_u(t)\hat{\mathbf{v}}_u^\perp + \frac{\alpha_u(t)\left(\hat{\mathbf{v}}_u \cdot \hat{\mathbf{v}}_s\right) - \alpha_s(t)}{\hat{\mathbf{v}}_u \wedge \hat{\mathbf{v}}_s} \hat{\mathbf{v}}_u \right] + \mathcal{O}(\varepsilon^2) \tag{2.25}$$

in terms of $\alpha_{u,s}(t)$ defined in (2.23).

Proof. See section 3.5. ■

Remark 2.11. The orthogonal system $\left(\hat{\mathbf{v}}_s, \hat{\mathbf{v}}_s^\perp\right)$ could be used alternatively in (2.25) by simply performing the interchange $u \leftrightarrow s$ throughout.

Remark 2.12. The behavior of $\mathbf{g}\left(\mathbf{a}, \cdot\right)$ on both semi-infinite lines $(-\infty, t)$ and (t, ∞) is needed to determine the location of the saddle at any fixed time t.

Remark 2.13. Theorem 2.10 provides an important tool in flow control [2, 62] for which the time-dependent hyperbolic trajectory may need to be controlled through an introduced perturbation $\mathbf{g}$.

Remark 2.14. While the location of the perturbed hyperbolic trajectory can be imputed using exponential dichotomies of a linearized equation [62], Theorem 2.10 provides a crisp formula for this process. The Laplace transform representation (2.23) enables quick computation using canned software packages and may be particularly relevant in control theoretical applications.

3. Proofs.

3.1. Proof of Theorem 2.1 (unstable manifold's normal displacement).

The proof here mirrors the intermediate stages of the proof of the Melnikov function by Guckenheimer and Holmes [26], and particularly by Holmes [32], in which the divergence-free nature of $\mathbf{f}$ is relaxed. However, the derivation will be presented in detail in the interests of coherence, since several adjustments are needed; such as the performance of the calculation at a movable point $\bar{\mathbf{x}}^u(p)$ rather than a fixed location, the emphasis on locating the manifold rather than distances between manifolds, the lack of necessity of a homoclinic connection, the legitimacy of discarding higher-order terms, and the potential divergence of the Melnikov expression. This last issue is also related to the possible divergence of a boundary term in going from (20) to (21) in Holmes [32]. Most geometric Melnikov developments following formal perturbative analysis [26, 4, 32] discard the $\mathcal{O}(\varepsilon)$ terms in the Melnikov integral, which actually needs additional consideration since an integration over a noncompact interval needs to be performed. All these issues are dealt with in this proof.

Begin by defining $\mathbf{x}_1^u$ by

$$\mathbf{x}_\varepsilon^u(p,\tau) = \bar{\mathbf{x}}^u(\tau - t + p) + \varepsilon\,\mathbf{x}_1^u(p,\tau,\varepsilon). \tag{3.1}$$

Given the $\mathcal{O}(\varepsilon)$-closeness of $\mathbf{x}_\varepsilon^u(p,\tau)$ and $\bar{\mathbf{x}}^u(\tau - t + p)$, this means that

$$|\mathbf{x}_1^u(p,\tau,\varepsilon)| \le K \quad \text{for } \tau \in [-\infty, T], \tag{3.2}$$

for a K independent of both τ and $\varepsilon \in [0,\varepsilon_0]$ for some ε_0. Now define the preliminary unstable Melnikov function by

$$M_\varepsilon^u(p,\tau) := \mathbf{f}\left(\bar{\mathbf{x}}^u(\tau - t + p)\right) \wedge \mathbf{x}_1^u(p,\tau,\varepsilon). \tag{3.3}$$

Note that

$$d^u(p,t,\varepsilon) = \varepsilon\,\hat{\mathbf{f}}^\perp\left(\bar{\mathbf{x}}^u(p)\right)\cdot \mathbf{x}_1^u(p,t,\varepsilon) = \varepsilon\,\frac{\mathbf{f}\left(\bar{\mathbf{x}}^u(p)\right)}{\left|\mathbf{f}\left(\bar{\mathbf{x}}^u(p)\right)\right|} \wedge \mathbf{x}_1^u(p,t,\varepsilon) = \varepsilon\,\frac{M_\varepsilon^u(p,t)}{\left|\mathbf{f}\left(\bar{\mathbf{x}}^u(p)\right)\right|}, \tag{3.4}$$

and hence $M_\varepsilon^u(p,t)$ carries information on the movement of the manifold in the direction perpendicular to $\mathbf{f}(\bar{\mathbf{x}}^u(p))$. Taking the derivative of $M_\varepsilon^u(p,\tau)$ in (3.3) with respect to τ (at fixed t and p),

$$\begin{aligned}
\frac{\partial M_\varepsilon^u}{\partial \tau} &= \left[D\mathbf{f}\left(\bar{\mathbf{x}}^u(\tau-t+p)\right)\frac{\partial \bar{\mathbf{x}}^u(\tau-t+p)}{\partial\tau}\right] \wedge \mathbf{x}_1^u(p,\tau,\varepsilon) \\
&\quad + \mathbf{f}\left(\bar{\mathbf{x}}^u(\tau-t+p)\right) \wedge \frac{\partial \mathbf{x}_1^u(p,\tau,\varepsilon)}{\partial\tau} \\
&= \left[D\mathbf{f}\left(\bar{\mathbf{x}}^u(\tau-t+p)\right)\mathbf{f}\left(\bar{\mathbf{x}}^u(\tau-t+p)\right)\right] \wedge \mathbf{x}_1^u(p,\tau,\varepsilon) \\
&\quad + \mathbf{f}\left(\bar{\mathbf{x}}^u(\tau-t+p)\right) \wedge \frac{\left[\mathbf{f}\left(\mathbf{x}_\varepsilon^u(p,\tau)\right) + \varepsilon\mathbf{g}\left(\mathbf{x}_\varepsilon^u(p,\tau),\tau\right) - \mathbf{f}\left(\bar{\mathbf{x}}^u(\tau-t+p)\right)\right]}{\varepsilon} \\
&= \left[D\mathbf{f}\left(\bar{\mathbf{x}}^u(\tau-t+p)\right)\mathbf{f}\left(\bar{\mathbf{x}}^u(\tau-t+p)\right)\right] \wedge \mathbf{x}_1^u(p,\tau,\varepsilon) \\
&\quad + \mathbf{f}\left(\bar{\mathbf{x}}^u(\tau-t+p)\right) \wedge \left[D\mathbf{f}\left(\bar{\mathbf{x}}^u(\tau-t+p)\right)\mathbf{x}_1^u(p,\tau,\varepsilon)\right] \\
&\quad + \mathbf{f}\left(\bar{\mathbf{x}}^u(\tau-t+p)\right) \wedge \mathbf{g}\left(\bar{\mathbf{x}}^u(\tau-t+p),\tau\right) \\
&\quad + \varepsilon\,\mathbf{f}\left(\bar{\mathbf{x}}^u(\tau-t+p)\right) \wedge \left[\frac{1}{2}\mathbf{x}_1^u(p,\tau,\varepsilon)^T D^2\mathbf{f}\left(\mathbf{y}_1\right) + D\mathbf{g}\left(\mathbf{y}_2,\tau\right)\right]\mathbf{x}_1^u(p,\tau,\varepsilon)\,.
\end{aligned} \tag{3.5}$$

The initial steps in the above calculations have utilized the facts that $\bar{\mathbf{x}}^u(\tau-t+p)$ is a solution to (2.1) when $\varepsilon=0$, and $\mathbf{x}^u_\varepsilon(p,\tau)$ is similarly a solution when $\varepsilon \neq 0$. The final step arises from the error terms in Taylor's theorem, and $\mathbf{y}_1$ and $\mathbf{y}_2$ are vectors located within εK of $\bar{\mathbf{x}}^u(\tau-t+p)$. The following easily verifiable identity for 2×2 matrices A and 2×1 vectors $\mathbf{b}$ and $\mathbf{c}$ will be useful:

$$(A\,\mathbf{b})\wedge\mathbf{c}+\mathbf{b}\wedge(A\,\mathbf{c}) = (\mathrm{Tr}\,A)\;(\mathbf{b}\wedge\mathbf{c})\,.$$

Choosing $A = D\mathbf{f}\left(\bar{\mathbf{x}}^u(\tau-t+p)\right)$, $\mathbf{b}=\mathbf{f}\left(\bar{\mathbf{x}}^u(\tau-t+p)\right)$, and $\mathbf{c}=\mathbf{x}^u_1(p,\tau,\varepsilon)$ enables (3.5) to be written as

$$\begin{aligned}\frac{\partial M^u_\varepsilon}{\partial \tau} &= \nabla\cdot\mathbf{f}\left(\bar{\mathbf{x}}^u(\tau-t+p)\right)M^u_\varepsilon + \mathbf{f}\left(\bar{\mathbf{x}}^u(\tau-t+p)\right)\wedge\mathbf{g}\left(\bar{\mathbf{x}}^u(\tau-t+p),\tau\right)\\ &\quad+\varepsilon\,\mathbf{f}\left(\bar{\mathbf{x}}^u(\tau-t+p)\right)\wedge\left[\frac{1}{2}\mathbf{x}^u_1(p,\tau,\varepsilon)^T D^2\mathbf{f}\left(\mathbf{y}_1\right)+D\mathbf{g}\left(\mathbf{y}_2,\tau\right)\right]\mathbf{x}^u_1\left(p,\tau,\varepsilon\right).\end{aligned} \tag{3.6}$$

Suppose $M^u(p,\tau)$ satisfies the same boundary condition at $\tau\to-\infty$ as $M^u_\varepsilon(p,\tau)$, namely, that $M^u\to 0$, and that M^u solves (3.6), in which the ε-term is ignored; that is,

$$\frac{\partial M^u}{\partial\tau} = \nabla\cdot\mathbf{f}\left(\bar{\mathbf{x}}^u(\tau-t+p)\right)M^u+\mathbf{f}\left(\bar{\mathbf{x}}^u(\tau-t+p)\right)\wedge\mathbf{g}\left(\bar{\mathbf{x}}^u(\tau-t+p),\tau\right). \tag{3.7}$$

The solution of this linear equation for M^u involves using the integrating factor

$$\mu(\tau) := \exp\left[-\int_0^\tau \nabla\cdot\mathbf{f}\left(\bar{\mathbf{x}}^u(\xi-t+p)\right)\,\mathrm{d}\xi\right],$$

after which one obtains

$$\frac{\partial}{\partial\tau}\left[\mu(\tau)M^u(p,\tau)\right] = \mu(\tau)\mathbf{f}\left(\bar{\mathbf{x}}^u(\tau-t+p)\right)\wedge\mathbf{g}\left(\bar{\mathbf{x}}^u(\tau-t+p),\tau\right). \tag{3.8}$$

Integration of (3.8) from L to t leads to

$$\mu(t)M^u(p,t)-\mu(L)M^u(p,L)=\int_L^t\mu(\tau)\mathbf{f}\left(\bar{\mathbf{x}}^u(\tau-t+p)\right)\wedge\mathbf{g}\left(\bar{\mathbf{x}}^u(\tau-t+p),\tau\right)\mathrm{d}\tau. \tag{3.9}$$

The second term is indeterminate in the limit $L\to-\infty$, since the integrating factor μ is generically unbounded. However, note that

$$\left|\mu(L)M^u(p,L)\right| = \left|\mathbf{f}\left(\bar{\mathbf{x}}^u(L-t+p)\right)\wedge\mathbf{x}^u_1(L)\right|\exp\left[\int_L^0\nabla\cdot\mathbf{f}\left(\bar{\mathbf{x}}^u(\xi-t+p)\right)\,\mathrm{d}\xi\right].$$

Since $\mathbf{f}$ converges to zero exponentially (with rate λ_u) in this limit while $\mathbf{x}^u_1$ remains bounded, the wedge product can be bounded by $K_1e^{\lambda_u L}$, where K_1 is a constant. On the other hand, the integrand of μ approaches $\lambda_u+\lambda_s$ in this limit, since this is the sum of the eigenvalues at the limiting point $\mathbf{a}$. Thus, μ is bounded by $K_2e^{-(\lambda_u+\lambda_s)L}$. Hence

$$\lim_{L\to-\infty}\left|\mu(L)M^u(p,L)\right| \leq \lim_{L\to-\infty}K_1K_2e^{-\lambda_s L} = 0$$

since $\lambda_s < 0$. For completeness, the convergence of the integral in (3.9) is now examined. The term $|\mathbf{f} \wedge \mathbf{g}|$ is bounded by $K_3 e^{\lambda_u \tau}$ since $\mathbf{f}$ has exponential decay to zero and $\mathbf{g}$ is bounded, and μ is bounded by $K_2 e^{-(\lambda_u+\lambda_s)\tau}$, as mentioned previously. Thus, the integrand is bounded by $K_3 K_2 e^{-\lambda_s \tau}$, which is integrable over $(-\infty, 0)$. Thus, taking the limit $L \to -\infty$ in (3.9) yields

(3.10)
$$M^u(p,t) = \int_{-\infty}^{t} \exp\left[\int_{\tau}^{t} \nabla \cdot \mathbf{f}\left(\bar{\mathbf{x}}^u(\xi - t + p)\right) \mathrm{d}\xi\right] \mathbf{f}\left(\bar{\mathbf{x}}^u(\tau - t + p)\right) \wedge \mathbf{g}\left(\bar{\mathbf{x}}^u(\tau - t + p), \tau\right) \mathrm{d}\tau,$$

in which the improper integral converges. The change of variable $\tau - t + p \to \tau$ results in (2.7).

It remains to show that the solution to (3.6) is within $\mathcal{O}(\varepsilon)$ of (3.7), which is not obvious since integration over the noncompact domain $(-\infty, t)$ is needed for the solution. Subtracting (3.7) from (3.6) gives

$$\frac{\partial}{\partial \tau}\left[M^u_\varepsilon - M^u\right] = \varepsilon\, \mathbf{f} \wedge \left[\frac{1}{2}\mathbf{x}^u_1(p,\tau,\varepsilon)^T D^2 \mathbf{f}\left(\mathbf{y}_1\right) + D\mathbf{g}\left(\mathbf{y}_2, \tau\right)\right] \mathbf{x}^u_1, \tag{3.11}$$

where (when omitted) the spatial argument is $\bar{\mathbf{x}}^u(\tau - t + p)$ and the temporal argument is τ. When considering $\tau \in (-\infty, t)$, $\mathbf{x}^u_1(p,\tau,\varepsilon)$ remains bounded by K. The matrix $D^2\mathbf{f}(\mathbf{y}_1)$ also remains bounded, since $\mathbf{y}_1$ lies within εK of points in the unstable manifold segment $\bar{\mathbf{x}}^u(\tau - t + p)$ and thus can be forced to lie on a compact set. A similar argument works for the first argument of $D\mathbf{g}\left(\mathbf{y}_2, \tau\right)$, and the second argument offers no difficulty since it is assumed that $D\mathbf{g}$ is bounded in time as well. The prefactor term $\mathbf{f}\left(\bar{\mathbf{x}}^u(\tau - t + p)\right)$ has a stronger bound because of the exponential decay with rate λ_u. Thus, there exists a constant K_4 such that the right-hand side of (3.11) is bounded by a term $\varepsilon K_4 e^{\lambda_u \tau}$. Hence

$$-\varepsilon K_4 e^{\lambda_u \tau} \le \frac{\partial}{\partial \tau}\left[M^u_\varepsilon(p,\tau,\varepsilon) - M^u(p,\tau)\right] \le \varepsilon K_4 e^{\lambda_u \tau}.$$

Consider integrating the above from $-\infty$ to t and note from (3.3) that M^u_ε goes to zero as $\tau \to -\infty$, which M^u is also assumed to obey. This enables the bound

$$\left|M^u_\varepsilon(p,t) - M^u(p,t)\right| \le \varepsilon \frac{K_4}{\lambda_u} e^{\lambda_u t}, \tag{3.12}$$

and thus $M^u_\varepsilon(p,t) = M^u(p,t) + \mathcal{O}(\varepsilon)$. Applying this to (3.4) yields (2.6).

3.2. Proof of Theorem 2.3 (unstable manifold's tangential displacement). Define the "tangential version" of (3.3) by

$$B^u_\varepsilon(p,\tau) := \mathbf{f}\left(\bar{\mathbf{x}}^u(\tau - t + p)\right) \cdot \mathbf{x}^u_1(p,\tau,\varepsilon) = \mathbf{f}^T\left(\bar{\mathbf{x}}^u(\tau - t + p)\right) \mathbf{x}^u_1(p,\tau,\varepsilon). \tag{3.13}$$

Note from (2.8) that $\mathbf{x}^u_\varepsilon$ is chosen such that it is located in the direction of $\mathbf{f}^\perp$ with respect to $\bar{\mathbf{x}}(0)$ in the time-slice $t - p$, and hence $B^u_\varepsilon(p, t-p) = 0$. Now

$$c^u(p,t,\varepsilon) = \varepsilon\, \hat{\mathbf{f}}\left(\bar{\mathbf{x}}^u(p)\right) \cdot \mathbf{x}^u_1(p,t,\varepsilon) = \varepsilon \frac{B^u_\varepsilon(p,t)}{\left|\mathbf{f}\left(\bar{\mathbf{x}}^u(p)\right)\right|}. \tag{3.14}$$

Taking the τ-derivative of $B_\varepsilon^u(p,\tau)$ in (3.13) at fixed t and p, and utilizing the expression for the derivative of $\mathbf{x}_1^u$ as used in the derivation of (3.5), one obtains

$$\begin{aligned}\frac{\partial B_\varepsilon^u}{\partial \tau} &= \mathbf{f}^T\left(\bar{\mathbf{x}}^u(\tau-t+p)\right)\left[D\mathbf{f}\left(\bar{\mathbf{x}}^u(\tau-t+p)\right)\mathbf{x}_1^u(p,\tau,\varepsilon)+\mathbf{g}\left(\bar{\mathbf{x}}^u(\tau-t+p),\tau\right)\right]\\ &\quad+\frac{\partial \mathbf{f}^T\left(\bar{\mathbf{x}}^u(\tau-t+p)\right)}{\partial\tau}\mathbf{x}_1^u(p,\tau,\varepsilon)\\ &\quad+\varepsilon\,\mathbf{f}\left(\bar{\mathbf{x}}^u(\tau-t+p)\right)^T\left[\frac{1}{2}\mathbf{x}_1^u(p,\tau,\varepsilon)^T D^2\mathbf{f}\left(\mathbf{y}_1\right)+D\mathbf{g}\left(\mathbf{y}_2,\tau\right)\right]\mathbf{x}_1^u\left(p,\tau,\varepsilon\right),\end{aligned} \tag{3.15}$$

where $\mathbf{y}_{1,2}$ are as described in (3.5). Now note that

$$\begin{aligned}\frac{\partial \mathbf{f}\left(\bar{\mathbf{x}}^u(\tau-t+p)\right)}{\partial\tau} &= D\mathbf{f}\left(\bar{\mathbf{x}}^u(\tau-t+p)\right)\frac{\partial\bar{\mathbf{x}}^u(\tau-t+p)}{\partial\tau}\\ &= D\mathbf{f}\left(\bar{\mathbf{x}}^u(\tau-t+p)\right)\mathbf{f}\left(\bar{\mathbf{x}}^u(\tau-t+p)\right);\end{aligned}$$

i.e., $\mathbf{f}$ satisfies the equation of variation associated with (2.1) when $\varepsilon=0$. Therefore,

$$\frac{\partial}{\partial\tau}\mathbf{f}=\left(D\mathbf{f}\right)\mathbf{f} \quad \text{and} \quad \frac{\partial}{\partial\tau}\mathbf{f}^T=\mathbf{f}^T\left(D\mathbf{f}\right)^T \tag{3.16}$$

with each quantity being evaluated at $\bar{\mathbf{x}}^u(\tau-t+p)$. Substituting in (3.15),

$$\frac{\partial}{\partial\tau}\left[\mathbf{f}^T\mathbf{x}_1^u\right]=\mathbf{f}^T\left[(D\mathbf{f})^T+D\mathbf{f}\right]\mathbf{x}_1^u+\mathbf{f}^T\mathbf{g}+\varepsilon\,\mathbf{f}^T\left[\frac{1}{2}\left(\mathbf{x}_1^u\right)^T D^2\mathbf{f}\left(\mathbf{y}_1\right)+D\mathbf{g}\left(\mathbf{y}_2,\tau\right)\right]\mathbf{x}_1^u, \tag{3.17}$$

where (when omitted) the spatial arguments are $\bar{\mathbf{x}}^u(\tau-t+p)$ and the temporal argument is τ. Even if the ε-term were discarded, (3.17) is not a closed equation for $B^u=\mathbf{f}^T\mathbf{x}_1^u$, and the Melnikov strategy adopted for solving for M_ε^u cannot be used. Now note that $\mathbf{x}_1^u$ can be written in terms of its components in the two perpendicular directions $\hat{\mathbf{f}}$ and $\hat{\mathbf{f}}^\perp$ by

$$\mathbf{x}_1^u=\frac{\mathbf{f}^T\mathbf{x}_1^u}{|\mathbf{f}|}\hat{\mathbf{f}}+\frac{\mathbf{f}\wedge\mathbf{x}_1^u}{|\mathbf{f}|}\hat{\mathbf{f}}^\perp=\frac{B_\varepsilon^u}{|\mathbf{f}|^2}\mathbf{f}+\frac{M_\varepsilon^u}{|\mathbf{f}|^2}\mathbf{f}^\perp.$$

With the definition of Ω^u in (2.10), (3.17) can be written as

$$\begin{aligned}\frac{\partial B_\varepsilon^u}{\partial\tau} &= \frac{\mathbf{f}^T\left[(D\mathbf{f})^T+D\mathbf{f}\right]\mathbf{f}}{|\mathbf{f}|^2}B_\varepsilon^u+\Omega^u(\tau-t+p)M_\varepsilon^u(p,\tau)+\mathbf{f}^T\mathbf{g}\\ &\quad+\varepsilon\,\mathbf{f}^T\left[\frac{1}{2}\left(\mathbf{x}_1^u\right)^T D^2\mathbf{f}\left(\mathbf{y}_1\right)+D\mathbf{g}\left(\mathbf{y}_2,\tau\right)\right]\mathbf{x}_1^u.\end{aligned} \tag{3.18}$$

The linear coefficient in (3.18) simplifies to

$$\frac{\mathbf{f}^T\left[(D\mathbf{f})^T+D\mathbf{f}\right]\mathbf{f}}{|\mathbf{f}|^2}=\frac{\frac{\partial\mathbf{f}^T}{\partial\tau}\mathbf{f}+\mathbf{f}^T\frac{\partial\mathbf{f}}{\partial\tau}}{|\mathbf{f}|^2}=\frac{\frac{\partial}{\partial\tau}\left[\mathbf{f}^T\mathbf{f}\right]}{|\mathbf{f}|^2}=\frac{1}{|\mathbf{f}|^2}\frac{\partial}{\partial\tau}|\mathbf{f}|^2=\frac{\partial}{\partial\tau}\left(\ln|\mathbf{f}|^2\right)$$

through the usage of the variational equations (3.16). Moreover,

$$\Omega^u(\tau-t+p)M_\varepsilon^u(p,\tau)=\Omega^u(\tau-t+p)M^u(p,\tau)+\Omega^u(\tau-t+p)\left[M_\varepsilon^u(p,\tau)-M^u(p,\tau)\right],$$

enabling (3.18) to become

$$\begin{aligned}\frac{\partial B_\varepsilon^u}{\partial\tau}&=\frac{\partial}{\partial\tau}\left(\ln|\mathbf{f}|^2\right)\,B_\varepsilon^u+\Omega^u(\tau-t+p)M^u(p,\tau)+\mathbf{f}^T\mathbf{g}\\&\quad+\varepsilon\,\mathbf{f}^T\left[\frac{1}{2}\left(\mathbf{x}_1^u\right)^T D^2\mathbf{f}\left(\mathbf{y}_1\right)+D\mathbf{g}\left(\mathbf{y}_2,\tau\right)\right]\mathbf{x}_1^u\\&\quad+\Omega^u(\tau-t+p)\left[M_\varepsilon^u(p,\tau)-M^u(p,\tau)\right].\end{aligned}\tag{3.19}$$

Now, the last two lines of (3.19) are $\mathcal{O}(\varepsilon)$ terms—a point which will be elaborated on later. Suppose $B^u(p,\tau)$ is the solution to the equation in which these terms are ignored, i.e.,

$$\frac{\partial B^u}{\partial\tau}=\frac{\partial}{\partial\tau}\left(\ln|\mathbf{f}|^2\right)\,B^u+\Omega^u(\tau-t+p)M^u(p,\tau)+\mathbf{f}^T\mathbf{g},\tag{3.20}$$

which moreover satisfies the same "initial" condition as B_ε^u, namely, $B^u(p,t-p)=0$. This has an integrating factor

$$\mu(\tau):=\exp\left[-\int_t^\tau\frac{\partial}{\partial u}\ln\left|\mathbf{f}\left(\bar{\mathbf{x}}^u(u-t+p)\right)\right|^2\mathrm{d}u\right]=\frac{\left|\mathbf{f}\left(\bar{\mathbf{x}}^u(p)\right)\right|^2}{\left|\mathbf{f}\left(\bar{\mathbf{x}}^u(\tau-t+p)\right)\right|^2};$$

using which (3.20) can be represented by

$$\frac{\partial}{\partial\tau}\left[\frac{B^u(p,\tau)}{\left|\mathbf{f}\left(\bar{\mathbf{x}}^u(\tau-t+p)\right)\right|^2}\right]=\frac{\Omega^u(\tau-t+p)M^u(p,\tau)+\mathbf{f}^T\mathbf{g}}{\left|\mathbf{f}\left(\bar{\mathbf{x}}^u(\tau-t+p)\right)\right|^2}.\tag{3.21}$$

While it is clear from (3.13) that $B^u\to 0$ as $\tau\to-\infty$, this condition cannot be applied to (3.21) because the denominator $|\mathbf{f}|^2$ also goes to zero (and indeed does so faster than the numerator). Hence, (3.21) cannot be integrated from $-\infty$ as was done for the normal component. This highlights the necessity of another condition at a finite time, which in this case is $B^u(p,t-p)=0$, as reflected in (2.8). Integrating (3.21) from $t-p$ to t, and utilizing $B^u(p,t-p)=0$,

$$\frac{B^u(p,t)}{\left|\mathbf{f}\left(\bar{\mathbf{x}}^u(p)\right)\right|^2}=\int_{t-p}^t\frac{\Omega^u(\tau-t+p)M^u(p,\tau)+\mathbf{f}^T\left(\bar{\mathbf{x}}^u(\tau-t+p)\right)\mathbf{g}\left(\bar{\mathbf{x}}^u(\tau-t+p),\tau\right)}{\left|\mathbf{f}\left(\bar{\mathbf{x}}^u(\tau-t+p)\right)\right|^2}\mathrm{d}\tau.$$

By changing the variable of integration in the form $\tau-t+p\to\tau$, (2.12) is obtained.

It remains to argue that the terms neglected in (3.19) yield higher-order corrections to B^u. The terms explicitly with an ε in front in (3.19) have a specific bound as argued in section 3.1, and since the integration here is over a finite interval, their contribution remains $\mathcal{O}(\varepsilon)$. The final term in (3.19) can be bounded by

$$\left|\Omega^u(\tau-t+p)\left[M_\varepsilon^u(p,\tau)-M^u(p,\tau)\right]\right|\le\varepsilon\left|\Omega^u(\tau-t+p)\right|\frac{K_4}{\lambda_u}e^{\lambda_u\tau}\le\varepsilon K_5 e^{\lambda_u\tau}$$

by using (3.12) at a general point τ, and then by realizing from (2.10) that Ω^u remains bounded since it approaches a constant in the limit as $\tau\to-\infty$ ($D\mathbf{f}$ converges to the local linearization at $\mathbf{a}$, and $\hat{\mathbf{f}}\to\hat{\mathbf{v}}_u$). Therefore, the contribution from this term also remains $\mathcal{O}(\varepsilon)$, implying that $B_\varepsilon^u(p,t)$ and $B^u(p,t)$ differ by at most $\mathcal{O}(\varepsilon)$. Applying this to (3.14) yields (2.11).

3.3. Proof of Theorem 2.7 (stable manifold's normal displacement). Adopt an expansion similar to (3.1),

$$\mathbf{x}_\varepsilon^s(p,\tau) = \bar{\mathbf{x}}^s(\tau - t + p) + \varepsilon\, \mathbf{x}_1^s(p,\tau,\varepsilon), \tag{3.22}$$

now valid for $\tau \in [T,\infty]$, and define $M_\varepsilon^s(p,t)$ analogously to $M_\varepsilon^u(p,t)$ in section 3.1. Following the same argument as in section 3.1, $M^s(p,t)$ also obeys (3.8). Integrating (3.8) from $\tau = t$ to L and taking the limit as $L \to \infty$ gives the desired result. The convergence argument and the legitimacy of neglecting the $\mathcal{O}(\varepsilon)$ terms are exactly as given for the proof of Theorem 2.1.

3.4. Proof of Theorem 2.8 (stable manifold's tangential displacement). This proof is identical to that of Theorem 2.3 as given in section 3.2.

3.5. Proof of Theorem 2.10 (hyperbolic trajectory location). Consider applying the limit $p \to -\infty$ to

$$\hat{\mathbf{f}}^\perp\left(\bar{\mathbf{x}}^u(p)\right) \cdot \left[\mathbf{x}_\varepsilon^u(p,t) - \bar{\mathbf{x}}^u(p)\right] = \varepsilon \frac{M^u(p,t)}{\left|\mathbf{f}\left(\bar{\mathbf{x}}^u(p)\right)\right|} + \mathcal{O}(\varepsilon^2).$$

The left-hand side converges to $\hat{\mathbf{v}}_u^\perp \cdot [\mathbf{a}_\varepsilon(t) - \mathbf{a}]$. In analyzing the limit on the $\mathcal{O}(\varepsilon)$ term on the right, it is convenient to represent M^u by employing the change of integration variable $\tau \to \tau - t + p$ as given in (3.10) in the proof of Theorem 3.1. The limit of this leading-order term is then

$$\begin{aligned}\Xi_u &= \lim_{p\to-\infty} \int_{-\infty}^{t} \exp\left[\int_\tau^t \nabla\cdot\mathbf{f}\left(\bar{\mathbf{x}}^u(\xi - t + p)\right)\mathrm{d}\xi\right] \frac{\mathbf{f}\left(\bar{\mathbf{x}}^u(\tau - t + p)\right)}{\left|\mathbf{f}\left(\bar{\mathbf{x}}^u(p)\right)\right|} \wedge \mathbf{g}\left(\bar{\mathbf{x}}^u(\tau - t + p),\tau\right)\mathrm{d}\tau \\ &= \lim_{p\to-\infty} \int_{-\infty}^{t} \exp\left[\int_\tau^t \nabla\cdot\mathbf{f}\left(\bar{\mathbf{x}}^u(\xi - t + p)\right)\mathrm{d}\xi\right] \frac{\left|\mathbf{f}\left(\bar{\mathbf{x}}^u(\tau - t + p)\right)\right|}{\left|\mathbf{f}\left(\bar{\mathbf{x}}^u(p)\right)\right|} \mathbf{g}_u^\perp\left(\bar{\mathbf{x}}^u(\tau - t + p),\tau\right)\mathrm{d}\tau,\end{aligned} \tag{3.23}$$

in which $\mathbf{g}_u^\perp$ is the component of $\mathbf{g}$ in the direction of $\hat{\mathbf{v}}_u^\perp$. Now, for suitably negative p, it is claimed that the integrand above is bounded by

$$H(\tau) := C\, e^{\lambda_s(t-\tau)}\, \mathbf{g}_u^\perp(\mathbf{a},\tau) \tag{3.24}$$

for some constant C. This claim works because of the hypotheses given at the beginning of section 2—the smoothness of $\mathbf{f}$ and the boundedness of $\mathbf{g}$. Since $\bar{\mathbf{x}}^u(\tau - t + p) \to \mathbf{a}$ exponentially as $p \to -\infty$, $\mathbf{g}_u^\perp$ remains bounded. Moreover, the quantity

$$\frac{\left|\mathbf{f}\left(\bar{\mathbf{x}}^u(\tau - t + p)\right)\right|}{\left|\mathbf{f}\left(\bar{\mathbf{x}}^u(p)\right)\right|} \to \frac{A\, e^{\lambda_u(\tau - t + p)}}{A\, e^{\lambda_u p}} = e^{\lambda_u(\tau - t)}$$

and thus can be bounded by a constant times the function on the right. Finally, $\nabla \cdot \mathbf{f} \to \operatorname{Tr} D\mathbf{f}(\mathbf{a}) = \lambda_u + \lambda_s$, and hence there exists K_4 such that

$$\exp\left[\int_\tau^t \nabla\cdot\mathbf{f}\left(\bar{\mathbf{x}}^u(\xi - t + p)\right)\mathrm{d}\xi\right] \le \exp\left[\int_\tau^t K_4\left(\lambda_u + \lambda_s\right)\mathrm{d}\xi\right] = e^{K_4} e^{(\lambda_u+\lambda_s)(t-\tau)}.$$

Putting these bounds together yields a bounding function of the form (3.24). Now, (3.24) is integrable over $(-\infty, t)$, and by the Lebesgue dominated convergence theorem, the limit $p \to$

$-\infty$ can be moved inside the integral in (3.23). Applying a term-by-term limit analogously to what has been described above,

$$\Xi_u = \int_{-\infty}^{t} \lim_{p\to-\infty} e^{(\lambda_u+\lambda_s)(t-\tau)} \frac{A\, e^{\lambda_u(\tau-t+p)}}{A\, e^{\lambda_u p}}\, \mathbf{g}_u^{\perp}(\mathbf{a},\tau)\, \mathrm{d}\tau = \int_{-\infty}^{t} e^{\lambda_s(t-\tau)} \mathbf{g}_u^{\perp}(\mathbf{a},\tau)\, \mathrm{d}\tau,$$

after which a straightforward shift in the integration variable yields the first equation in (2.23).

The second equation in (2.23) is obtained by applying the limit $p \to \infty$ to

$$\hat{\mathbf{f}}^{\perp}(\bar{\mathbf{x}}^s(p)) \cdot [\mathbf{x}_\varepsilon^s(p,t) - \bar{\mathbf{x}}^s(p)] = \varepsilon \frac{M^s(p,t)}{|\mathbf{f}(\bar{\mathbf{x}}^s(p))|} + \mathcal{O}(\varepsilon^2).$$

The details are analogous to the above proof and will be omitted.

Obtaining the expression (2.25) relies on applying straightforward geometry, since the projections of $\mathbf{a}_\varepsilon(t) - \mathbf{a}$ in the potentially nonorthogonal directions $\hat{\mathbf{v}}_u^{\perp}$ and $\hat{\mathbf{v}}_s^{\perp}$ are known via (2.23). The linear independence of $\mathbf{v}_u$ and $\mathbf{v}_s$ ensures that $\hat{\mathbf{v}}_u \wedge \hat{\mathbf{v}}_s \neq 0$. Once again, the details will be omitted.

Remark 3.1. The above calculations used the normal displacements as given in Theorems 2.1 and 2.3. It is *not* possible to use the tangential displacement expressions in Theorems 2.3 and 2.8 to arrive at the displacement of the saddle point, since, for example, using (2.11) and (2.12) gives a potentially divergent result as $p \to -\infty$. This is caused by the boundary term arising from integrating (3.21), $B^u(p, t-p)/|\mathbf{f}(\bar{\mathbf{x}}^u(p))|$, being indeterminate in this limit, and thus the expression (2.12) is valid strictly for finite p.

4. Duffing oscillator. The Duffing oscillator in the form as studied by Holmes and Whitley [33], Wiggins [57, 56], and Mancho and collaborators [39, 34] will be examined, and the location of the hyperbolic trajectory and its invariant manifolds will be computed using the results derived in this article. Consider

$$\ddot{x} - x + x^3 + \delta\,\dot{x} = \gamma\,\mathrm{force}(t), \tag{4.1}$$

in which the damping $\delta > 0$ and forcing $\gamma > 0$ are both considered small, and the dot denotes the time derivative. Significant research has been done on this equation, for example, in establishing chaotic motion when $\delta = 0$, $\mathrm{force}(t) = \cos t$, and $0 < \gamma \ll 1$ [33, 57, 56], or when periodic orbits are persistent [37, 55]. When $\delta = 0$ and $\gamma = 0$, the Duffing oscillator (4.1) can be written as

$$\left.\begin{aligned} \dot{x} &= y \\ \dot{y} &= x - x^3 \end{aligned}\right\}. \tag{4.2}$$

This is a Hamiltonian system possessing a "figure-of-eight" phase space structure, with a saddle point at the origin. See Figure 3, in which the stable and unstable manifolds of the origin are indicated in the form Γ_i^σ, in which $\sigma = u, s$, and i represents the quadrant into which that branch of manifold extends from the saddle point. The behavior of the saddle point and these associated manifolds when either γ or δ is turned on will be examined. In preparation for this, note that $\Gamma_1^u = \Gamma_4^s$ and $\Gamma_3^u = \Gamma_2^s$ form two homoclinic loops, and the symmetry of

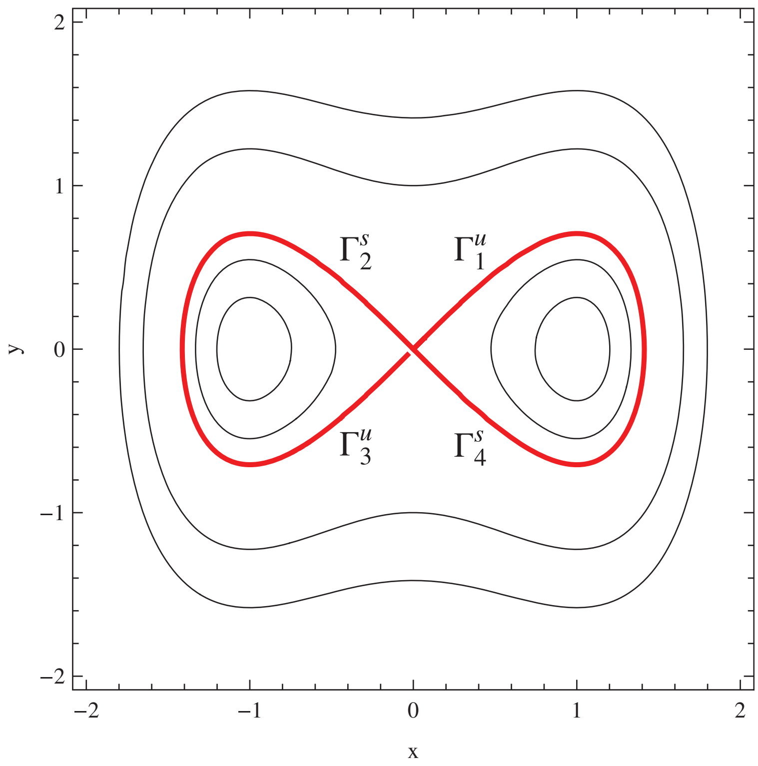

Figure 3. *Phase portrait of the undamped, unforced Duffing equation (4.2), with the saddle point at the origin and the four branches of its invariant manifolds in bold.*

the system ensures that it is sufficient to obtain information concerning the perturbation of $\Gamma_1^u = \Gamma_4^s$. This homoclinic manifold can be parametrized by

$$\bar{\mathbf{x}}(p) = \begin{pmatrix} \bar{x}(p) \\ \bar{y}(p) \end{pmatrix} = \begin{pmatrix} \sqrt{2}\,\text{sech}\ p \\ -\sqrt{2}\,\text{sech}\ p\ \tanh\ p \end{pmatrix}, \tag{4.3}$$

which works for either Γ_1^u or Γ_4^s. Straightforward linearization of the vector field $\mathbf{f} = \left(y, x - x^3\right)^T$ in (4.2) enables identification of the appropriate eigensystem at the origin to be

$$\lambda_u = 1\ ,\ \hat{\mathbf{v}}_u = \frac{1}{\sqrt{2}}\begin{pmatrix} 1 \\ 1 \end{pmatrix}; \qquad \lambda_s = -1\ ,\ \ \hat{\mathbf{v}}_s = \frac{1}{\sqrt{2}}\begin{pmatrix} -1 \\ 1 \end{pmatrix}.$$

The projected rate of strain associated with (4.2) along the homoclinic solution (4.3) is

$$\Omega^{u,s}(\tau) = \frac{\sqrt{2}\,(\cosh(2\tau) - 5)\,(3\cosh(2\tau) - 5)\ \text{sech}^5(\tau)}{\sqrt{9 - 6\cosh(2\tau) + \cosh(4\tau)}}.$$

4.1. No damping and small forcing.

When $\delta = 0$ and $0 < \gamma \ll 1$, (4.2) becomes

$$\left.\begin{aligned} \dot{x} &= y \\ \dot{y} &= x - x^3 + \gamma\,\text{force}(t) \end{aligned}\right\}, \tag{4.4}$$

in which γ is the small parameter, and $\mathbf{g} = (0, \text{force}(t))^T$. Thus,

$$\left.\begin{aligned} \mathbf{f}\left(\bar{\mathbf{x}}(\tau)\right) \wedge \mathbf{g}\left(\bar{\mathbf{x}}(\tau), \tau + t - p\right) &= \bar{y}(\tau)\, \text{force}\left(\tau + t - p\right) \\ \mathbf{f}\left(\bar{\mathbf{x}}(\tau)\right) \cdot \mathbf{g}\left(\bar{\mathbf{x}}(\tau), \tau + t - p\right) &= \left(\bar{x}(\tau) - [\bar{x}(\tau)]^3\right) \text{force}\left(\tau + t - p\right) \end{aligned}\right\}. \tag{4.5}$$

Since $\nabla \cdot \mathbf{f} = 0$, the expression for the unstable Melnikov function (2.7) simplifies. For a given forcing, it can be numerically (and, in some cases, analytically) calculated easily, and the unstable tangential function (2.12) can subsequently be numerically computed as well. The components of the saddle movement (2.24) are

$$\alpha_{\substack{u\\s}} = \frac{1}{\sqrt{2}} \mathcal{L}_\tau \left\{ \text{force}(t \mp \tau) \right\}(1) = \frac{1}{\sqrt{2}} \int_0^\infty \text{force}(t \mp \tau) e^{-\tau}\, \mathrm{d}\tau,$$

using the top and bottom signs, respectively, based on which the perturbed saddle location (2.25) is

$$\mathbf{a}(t) = \frac{\gamma}{2} \begin{pmatrix} -\displaystyle\int_0^\infty \left[\text{force}(t - \tau) + \text{force}(t + \tau)\right] e^{-\tau}\, \mathrm{d}\tau \\ \displaystyle\int_0^\infty \left[\text{force}(t - \tau) - \text{force}(t + \tau)\right] e^{-\tau}\, \mathrm{d}\tau \end{pmatrix} + \mathcal{O}(\gamma^2). \tag{4.6}$$

These expressions will now be used to compute the structures for the "standard" forcing $\text{force}(t) = \cos t$ [33, 57, 56] and then later for a time-aperiodic situation. If $\text{force}(t) = \cos t$, the above expressions enable the unstable Melnikov function to be written as

$$\begin{aligned} M^u(p,t) &= -\sqrt{2} \int_{-\infty}^{p} \operatorname{sech}(\tau) \tanh(\tau) \cos\left(\tau + t - p\right)\, \mathrm{d}\tau \\ &= -\sqrt{2} \Bigg[\cos t \int_{-\infty}^{p} \operatorname{sech}(\tau) \tanh(\tau) \cos\left(\tau - p\right)\, \mathrm{d}\tau \\ &\qquad - \sin t \int_{-\infty}^{p} \operatorname{sech}(\tau) \tanh(\tau) \sin\left(\tau - p\right)\, \mathrm{d}\tau \Bigg] \\ &= -\sqrt{2}\, A(p) \cos\left[t + \phi(p)\right], \end{aligned}$$

in which $A(p)$ and $\phi(p)$ are the modulus and argument of

$$\mathcal{G}(p) := e^{-ip} \int_{-\infty}^{p} \operatorname{sech}(\tau) \tanh(\tau)\, e^{i\tau}\, \mathrm{d}\tau = -\operatorname{sech}(p) + e^{p}(1+i)\, F\left(\frac{1+i}{2}, 1, \frac{3+i}{2}; -e^{2p}\right), \tag{4.7}$$

where the calculation was performed by dividing and multiplying by $A(p)$ following similar ideas [7, 6]. While the first equality in (4.7) defining $\mathcal{G}$ is adequate for computational purposes, the derivation of the alternative second form in terms of the hypergeometric function $F(a,b,c;z)$ as defined in (A.1) is relegated to Appendix A. It is clear from (2.12) that B^u is also periodic in t, but numerical evaluation is needed. Figure 4 shows a comparison between $M^u(0.35,t)$ and $B^u(0.35,t)$, which shows that the tangential and normal displacements of Γ_1^u

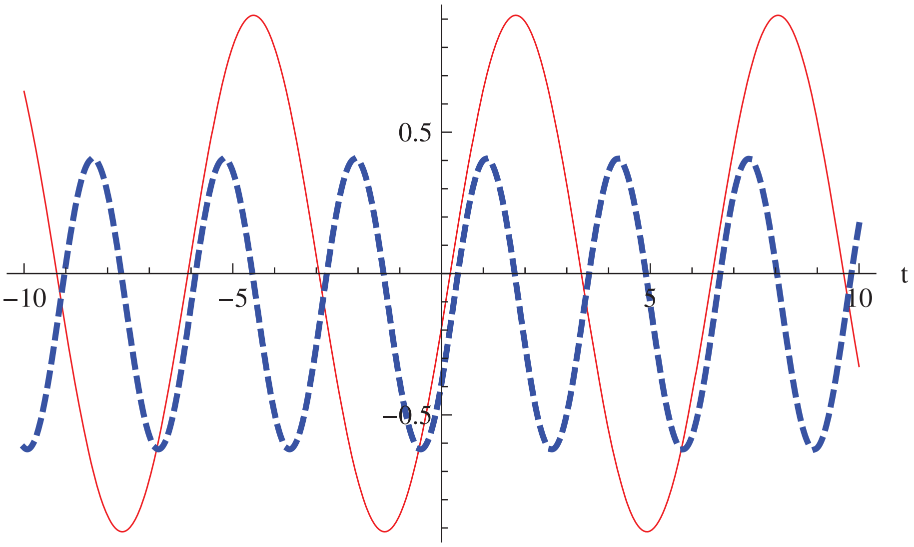

Figure 4. *$M^u(p,t)$ (solid) and $B^u(p,t)$ (dashed) for $p = 0.35$ in the case of no damping and small periodic forcing.*

are of comparable size at $p = 0.35$. The location of the perturbed manifold $\Gamma_1^u(\gamma)$ can be numerically determined by keeping only the $\mathcal{O}(\gamma)$ term in Remark 2.6. A numerical determination of this appears in Figure 5, which is drawn in the time-slice $t = 3$ for the choice of the small parameter $\gamma = 0.1$. The solid curve is the perturbed manifold, whereas the dashed curve is the unperturbed one. The dotted curve indicates the incorrect calculation for the perturbed unstable manifold that would occur if the tangential displacement were ignored. When picturing the manifold thus in a time-slice, the tangential displacement appears to give a less significant effect than the normal displacement for the obvious reason that moving a curve tangentially to itself by a small amount initially takes the point toward other points on the curve.

The locations of the other perturbed manifolds $\Gamma_4^s(\gamma)$, $\Gamma_2^s(\gamma)$, and $\Gamma_3^u(\gamma)$ can be obtained easily using symmetry. The intersections of these manifolds leads to chaotic motion but will not be analyzed since this is not the focus of this article. The location of the perturbed hyperbolic trajectory is from (4.6),

$$\mathbf{a}_\gamma(t) = \frac{\gamma}{2}\begin{pmatrix} -\cos t \\ \sin t \end{pmatrix} + \mathcal{O}(\gamma^2), \tag{4.8}$$

consistent with existing alternative derivations [34, 39].

Now, as a genuinely time-aperiodic example, consider

$$\text{force}(t) = \tanh t,$$

which transitions smoothly from a constant forcing in one direction to the other (an alternative, and much easier to compute, example would be the "switching on" of a force at a specific time, which could be modeled with the Heaviside function by $\text{force}(t) = H(t - t_0)$). Figures 6

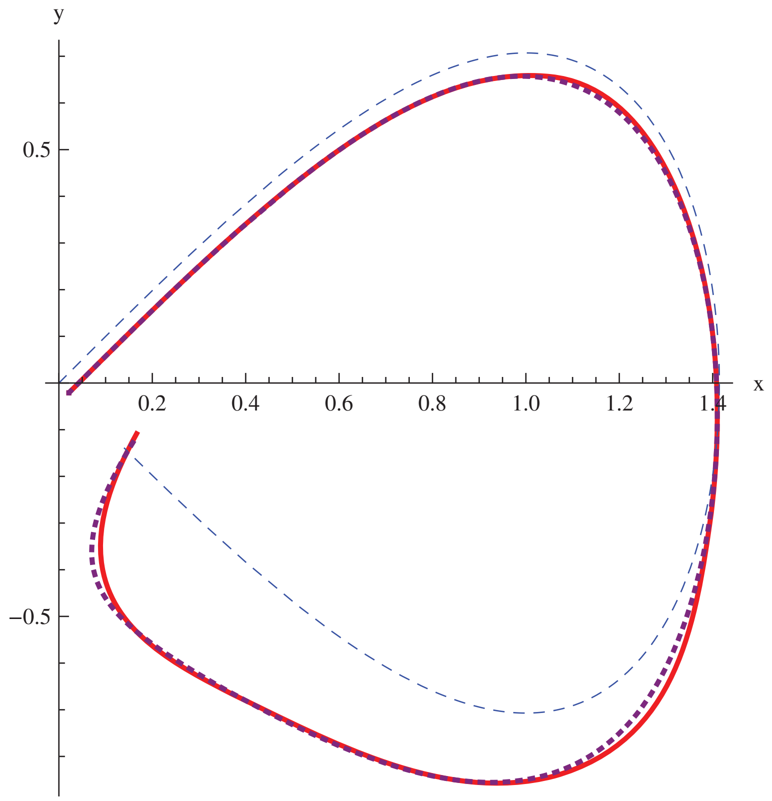

Figure 5. *Perturbed unstable manifold $\Gamma_1^u(\gamma)$ (solid) in the time-slice $t = 3$ in the case of no damping and periodic forcing with $\gamma = 0.1$, computed using Remark 2.6. The dashed curve is the unperturbed manifold, while the dotted curve is that computed by ignoring the tangential displacement.*

and 7 display numerically computed M^u and B^u variations, and it is apparent that B^u is of the same order as M^u and cannot be legitimately ignored. The corresponding unstable manifold in the time-slice $t = -3$ is shown in Figure 8. The fully three-dimensional unstable manifold $\Gamma_1^u(\gamma)$ computed to leading order in γ is shown in Figure 9. Such calculations can be performed in a straightforward manner for any reasonable forcing function, providing a new tool for analysis of arbitrary forcing in the Duffing equation to complement existing numerical algorithms [39].

The time variation of the perturbed hyperbolic trajectory can be explicitly determined using (4.6) and is

$$\mathbf{a}_\gamma(t) = \gamma \begin{pmatrix} e^{-t}\tan^{-1} e^t - e^t \cot^{-1} e^t \\ 1 - e^{-t}\tan^{-1} e^t - e^t \cot^{-1} e^t \end{pmatrix} + \mathcal{O}(\gamma^2). \tag{4.9}$$

In the limit $t \to -\infty$, the leading-order location approaches $(\gamma, 0)$, while it approaches $(-\gamma, 0)$ as $t \to \infty$. It was possible to compute this behavior with hardly any effort using Theorem 2.10. The leading-order locus of this hyperbolic trajectory is shown in Figure 10 for $\gamma = 0.1$; it progresses from $(-0.1, 0)$ to $(0.1, 0)$ as time varies from $-\infty$ to ∞.

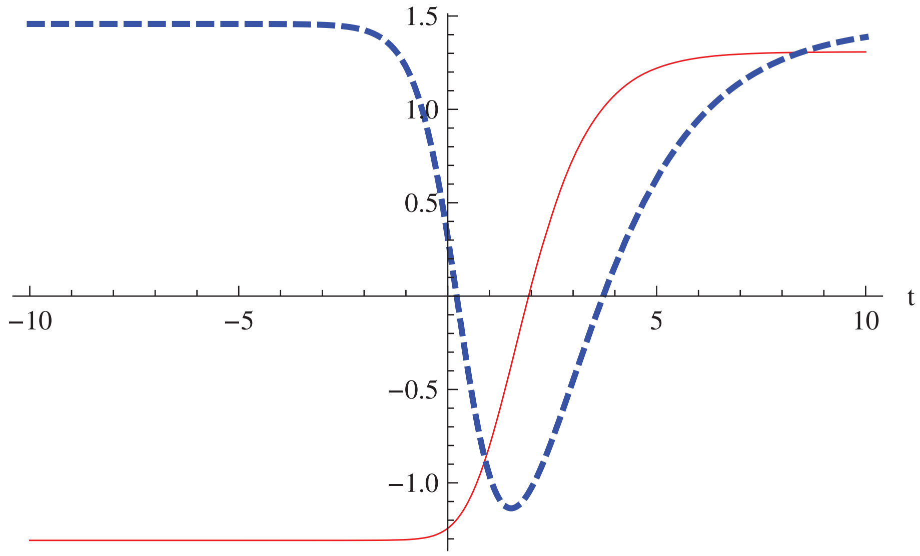

Figure 6. *$M^u(p,t)$ (solid) and $B^u(p,t)$ (dashed) for $p = 0.4$ in the case of no damping and with* $\mathrm{force}(t) = \tanh t$.

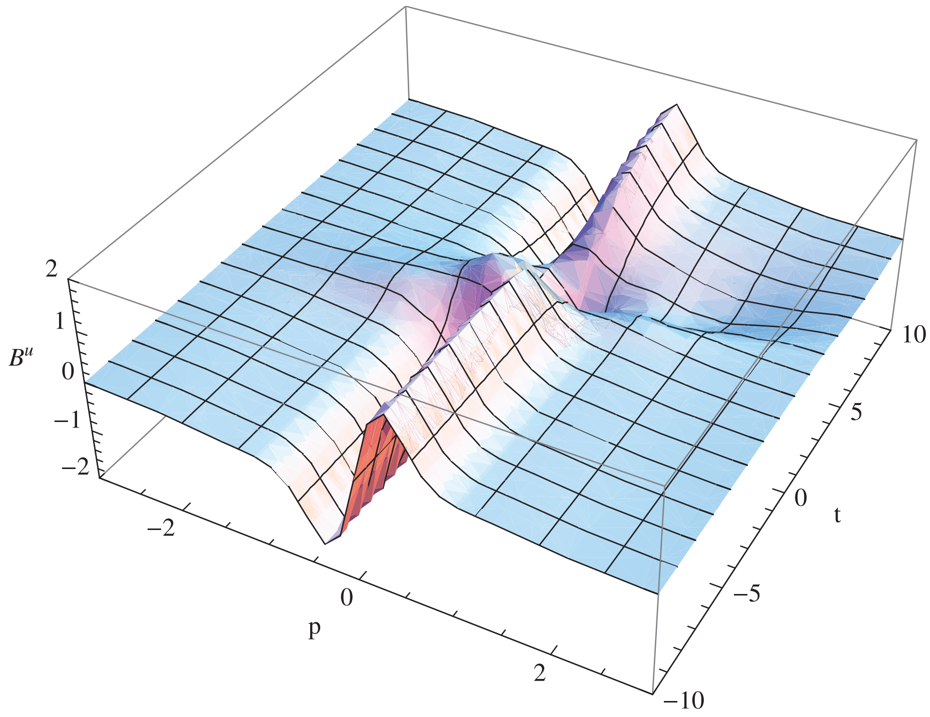

Figure 7. *$B^u(p,t)$ for $\delta = 0$ and* $\mathrm{force}(t) = \tanh t$.

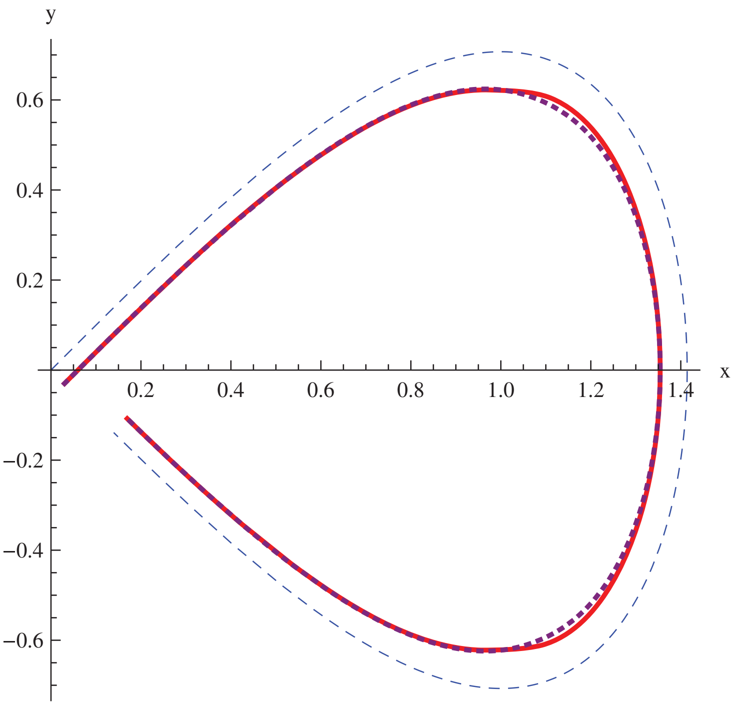

Figure 8. *Perturbed unstable manifold* $\Gamma_1^u(\gamma)$ *(solid) in the time-slice* $t = -3$*, in which* $\delta = 0$, $\text{force}(t) = \tanh t$*, and* $\gamma = 0.06$*, computed using Remark* 2.6*. The unperturbed manifold (dashed) and the incorrect manifold obtained by ignoring the tangential displacement (dotted) are also shown.*

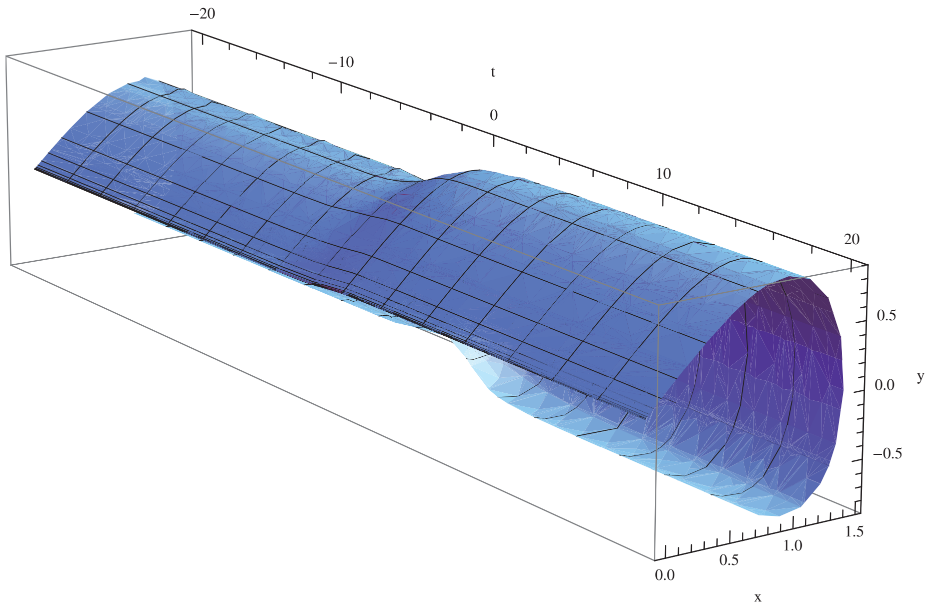

Figure 9. *Perturbed unstable manifold* $\Gamma_1^u(\gamma)$ *in the augmented* (x, y, t) *phase space for* $\delta = 0$, $\gamma = 0.1$*, and* $\text{force}(t) = \tanh t$*, computed using Remark* 2.6*.*

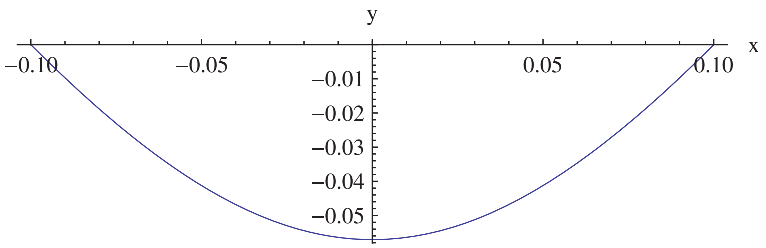

Figure 10. *The time variation of the perturbed hyperbolic trajectory when* $\delta = 0$, $\gamma = 0.1$, *and* $\mathrm{force}(t) = \tanh t$.

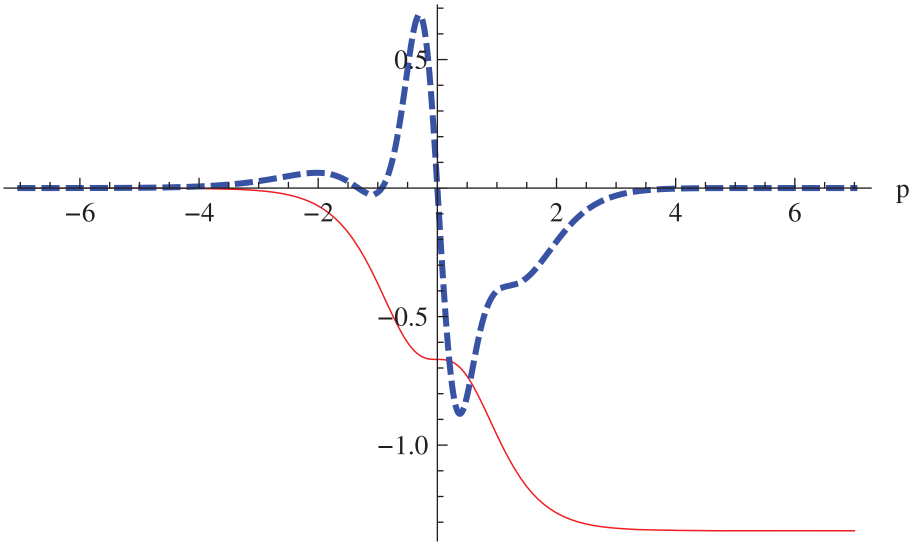

Figure 11. $M^u(p)$ *(solid) and* $B^u(p)$ *(dashed) for the situation of no forcing but small damping.*

4.2. No forcing and small damping.

When $\gamma = 0$ and $0 < \delta \ll 1$, (4.2) becomes

$$\left.\begin{aligned} \dot{x} &= y \\ \dot{y} &= x - x^3 - \delta y \end{aligned}\right\}, \tag{4.10}$$

which is well understood since it is autonomous and possesses a Lyapunov function [57]. Nevertheless, it is instructive to apply the results of this article to this situation. The unstable Melnikov function $M^u(p,t)$ is easily seen from (2.7) to be independent of t in this autonomous situation and is

$$M^u(p) = -\int_{-\infty}^{p} [\bar{y}(\tau)]^2 \, \mathrm{d}\tau = -2\int_{-\infty}^{p} \mathrm{sech}^2\tau \tanh^2\tau \, \mathrm{d}\tau = -\frac{2}{3}\left[1 + \tanh^3 p\right].$$

Inspection of (2.12) reveals that $B^u(p,t)$ also inherits this independence, as must happen since the perturbed system is also autonomous. A comparison of $M^u(p)$ with the numerically evaluated $B^u(p)$ appears in Figure 11. The function B^u here has significant contribution only in a localized region of p. However, as $M^u \to 1$ as $p \to \infty$, the perturbative expansion in ε given in (2.6) loses control as one proceeds along the manifold.

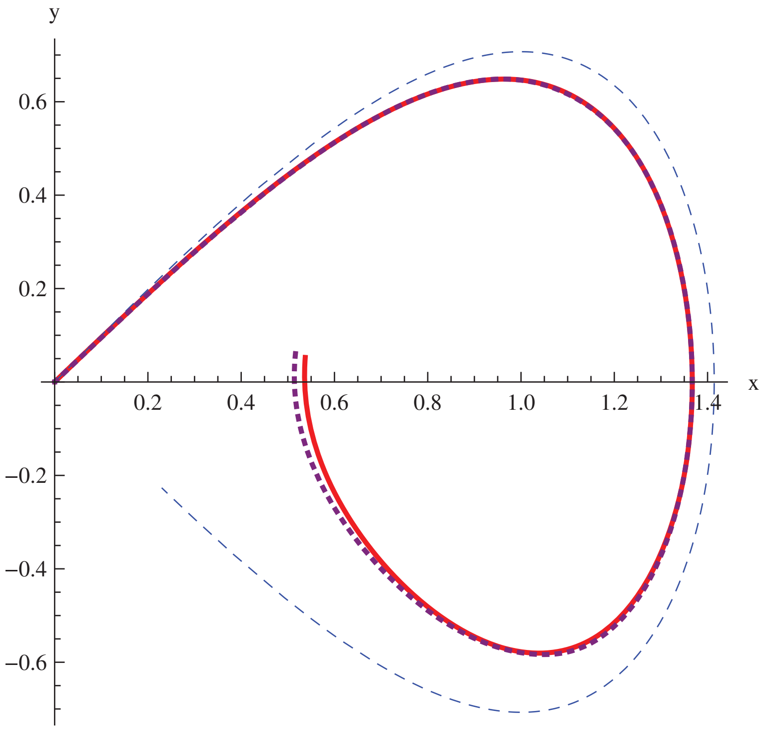

Figure 12. *The manifold $\Gamma_1^u(\delta)$ (solid) in the unforced Duffing equation computed using Remark 2.6 with $\delta = 0.1$. The unperturbed (undamped) manifold (dashed) and the incorrect manifold obtained by omitting the tangential displacement (dotted) are also pictured.*

The corresponding manifold $\Gamma_1^u(\delta)$ appears as the solid curve in Figure 12, where, as in Figure 8, the dashed curve is the unperturbed manifold and the dotted one the incorrect calculation of the perturbed manifold if the tangential component is ignored. The manifold wraps inward, as is well known, but how much it bends inward is underestimated if only the normal displacement is used.

If using Theorem 2.10 to calculate the displacement of the saddle point in this autonomous situation, both α_u and α_s turn out to be zero to leading order in δ. This is comforting, since it is clear from (4.10) that the saddle point continues to be at the origin.

5. Concluding remarks. The *normal* displacement between perturbed invariant manifolds, associated with the function of Melnikov [40], has been the main focus in the geometric analysis of invariant manifolds in the existing literature. A possible motivation for this is its connection to manifold intersections and chaos [26, 4, 57]. A wide range of applications exists: in oscillations [32, 51, 56, 33, 61, 59], in fluid transport [3, 48, 46, 29, 13, 7, 8, 10, 5], and recently also in combustion [12, 15] and in ecology [11, 9]. A pleasing theoretical formulation of manifold intersections in terms of a Lyapunov–Schmidt reduction [17, 44, 16, 14] also yields an alternative derivation of the Melnikov function, though its geometric meaning as a leading-order normal displacement is hidden with this approach. The existing (most general) normal displacement from a geometric perspective [32] suggests the correct formula, which was reaffirmed in the present article.

In contrast, the *tangential* displacement has never been studied. While not related to manifold intersections, this is still interesting both mathematically and from an applied perspective. The nonclosed nature of the equation arising from mimicking the geometric Melnikov approach implies that additional theoretical work was needed and has been provided in this article. The extant literature also provides no clues as to whether the presence of a tangential displacement was even known to exist, and that it was not possible to find the leading-order displacement of the manifolds with only "normal" information. However, as demonstrated in Figures 4 and 6 the tangential displacement may be as large as the normal displacement in some instances, and ignoring it is not justifiable. This article is thus the first to truly enable the computation of the perturbed manifold in the general time-aperiodic setting. There are immediate applications in geophysical fluid mechanics, in which determining time-dependent flow separators in barotropic (weakly two-dimensional) flows has been a significant research area for some time [43, 29, 46, 39, 13, 50, 24, 47, 28, 45, 52, 35]. Recent work by the author and collaborators in traveling wave problems in combustion and ecology [12, 15, 11, 9] yields another application: determining the perturbation to the traveling wave profile by applying the theory to the time-autonomous situation. Since a traveling wave is exactly associated with a heteroclinic trajectory, determining the perturbation to such a trajectory (i.e., determining the location of the persistent heteroclinic manifold) provides a direct method of quantifying the perturbation to the wave profile. The relaxation of area-preservation is particularly important in these traveling wave situations, since the governing reaction-diffusion equations generically yield non-Hamiltonian ordinary differential equations.

A side result in this article is the Laplace transform method for locating the perturbed hyperbolic trajectory ("moving saddle stagnation point"). The ease of use of the formulæ in Theorem 2.10 should make this a significant new tool in many applied areas. Once again, geophysical flows are an obvious application. There is also strong potential for using this tool in flow control theory [2] in determining perturbations which control the location of the time-dependent analogue of a stagnation point. Being presented in the language of Laplace transforms renders it particularly attractive to control theory.

Appendix A. Derivation of (4.7). This section outlines the derivation of the second equality in (4.7), in which the unstable Melnikov function associated with time-sinusoidal forcing of the Duffing equation is given in terms of the Gauss hypergeometric function F. This function can be expressed in terms of Euler's integral form [1] as

$$F(a,b,c;z) = \frac{\Gamma(c)}{\Gamma(a)\Gamma(c-a)} \int_0^1 \frac{s^{a-1}(1-s)^{c-a-1}}{(1-zs)^b} \mathrm{d}s, \tag{A.1}$$

in which Γ is the Gamma function. Now, the integral in the definition for $\mathcal{G}$ in (4.7) can be expressed as

$$\begin{aligned}\int_{-\infty}^{p} \operatorname{sech}\tau \tanh\tau\, e^{i\tau}\mathrm{d}\tau &= \int_{-\infty}^{p} \sinh\tau \operatorname{sech}^2\tau\, e^{i\tau}\mathrm{d}\tau \\ &= \left[\cosh\tau \operatorname{sech}^2\tau\, e^{i\tau}\right]_{-\infty}^{p} - \int_{-\infty}^{p} \cosh\tau\left(-2\operatorname{sech}^2\tau\tanh\tau + i\operatorname{sech}^2\tau\right)e^{i\tau}\mathrm{d}\tau \\ &= \operatorname{sech} p\, e^{ip} + 2\int_{-\infty}^{p} \operatorname{sech}\tau\tanh\tau\, e^{i\tau}\mathrm{d}\tau - \int_{-\infty}^{p} i\operatorname{sech}\tau\, e^{i\tau}\mathrm{d}\tau.\end{aligned}$$

Hence

$$
\begin{aligned}
\int_{-\infty}^{p} \operatorname{sech}\tau \tanh\tau \, e^{i\tau} \mathrm{d}\tau &= -\operatorname{sech} p \, e^{ip} + i \int_{-\infty}^{p} \operatorname{sech}\tau e^{i\tau} \mathrm{d}\tau \\
&= -\operatorname{sech} p \, e^{ip} + i \int_{-\infty}^{p} \frac{2e^{(1+i)\tau}}{e^{2\tau}+1} \mathrm{d}\tau \\
&= -\operatorname{sech} p \, e^{ip} + i e^{(1+i)p} \int_{0}^{1} \frac{s^{(-1+i)/2}}{1+e^{2p}s} \mathrm{d}s \\
&= -\operatorname{sech} p \, e^{ip} + i\,(1-i)\, e^{(1+i)p} F\left(\frac{1+i}{2}, 1, \frac{3+i}{2}; -e^{2p}\right),
\end{aligned}
$$

where the third equality is based on the substitution $s = e^{2(\tau-p)}$ and the last uses (A.1), since

$$
\frac{\Gamma\left(\frac{1+i}{2}\right)\Gamma(1)}{\Gamma\left(\frac{3+i}{2}\right)} = \frac{2}{1+i} = 1-i.
$$

Substitution into (4.7) leads to the required result.

Acknowledgments. I blame this article on Gary Froyland's manifold problems, and particularly on Georg Gottwald's (ab)normal scepticism, which led me tangentially. Thanks also to an anonymous referee's computer-algebra-free derivation of equation (4.7), as given in Appendix A.

REFERENCES

[1] M. Abramowitz and I. Stegun, *Handbook of Mathematical Functions*, National Bureau of Standards, Washington DC, 1972.

[2] F. Arai, A. Ichikawa, T. Fukuda, K. Horio, and K. Itoigawa, *Stagnation point control by pressure balancing in microchannel for high speed and high purity separation of microobject*, in Proceedings of the 2001 IEEE/RSJ International Conference on Intelligent Robots and Systems, Maui, HI, 2001, pp. 1343–1348.

[3] H. Aref, *Stirring by chaotic advection*, J. Fluid Mech., 143 (1984), pp. 1–21.

[4] D. Arrowsmith and C. Place, *An Introduction to Dynamical Systems*, University of Cambridge Press, Cambridge, UK, 1990.

[5] S. Balasuriya, *Approach for maximizing chaotic mixing in microfluidic devices*, Phys. Fluids, 17 (2005), 118103.

[6] S. Balasuriya, *Direct chaotic flux quantification in perturbed planar flows: General time-periodicity*, SIAM J. Appl. Dyn. Syst., 4 (2005), pp. 282–311.

[7] S. Balasuriya, *Optimal perturbation for enhanced chaotic transport*, Phys. D, 202 (2005), pp. 155–176.

[8] S. Balasuriya, *Cross-separatrix flux in time-aperiodic and time-impulsive flows*, Nonlinearity, 19 (2006), pp. 2775–2795.

[9] S. Balasuriya, *Invasions with density-dependent ecological parameters*, J. Theoret. Biol., 266 (2010), pp. 657–666.

[10] S. Balasuriya, *Optimal frequency for microfluidic mixing across a fluid interface*, Phys. Rev. Lett., 105 (2010), 064501.

[11] S. Balasuriya and G. Gottwald, *Wavespeed in reaction-diffusion systems, with applications to chemotaxis and population pressure*, J. Math. Biol., 61 (2010), pp. 377–399.

[12] S. Balasuriya, G. Gottwald, J. Hornibrook, and S. Lafortune, *High Lewis number combustion wavefronts: A perturbative Melnikov analysis*, SIAM J. Appl. Math., 67 (2007), pp. 464–486.

[13] S. Balasuriya, C. Jones, and B. Sandstede, *Viscous perturbations of vorticity-conserving flows and separatrix splitting*, Nonlinearity, 11 (1998), pp. 47–77.
[14] S. Balasuriya, I. Mezić, and C. Jones, *Weak finite-time Melnikov theory and 3D viscous perturbations of Euler flows*, Phys. D, 176 (2003), pp. 82–106.
[15] S. Balasuriya and V. Volpert, *Wavespeed analysis: Approximating Arrhenius kinetics with step-function kinetics*, Combust. Theor. Model., 12 (2008), pp. 643–670.
[16] F. Battelli and C. Lazzari, *Exponential dichotomies, heteroclinic orbits and Melnikov functions*, J. Differential Equations, 86 (1986), pp. 342–366.
[17] S.-N. Chow, J. Hale, and J. Mallet-Paret, *An example of bifurcation to homoclinic orbits*, J. Differential Equations, 37 (1980), pp. 351–373.
[18] W. A. Coppel, *Dichotomies in Stability Theory*, Lecture Notes in Math. 629, Springer-Verlag, Berlin, 1978.
[19] N. Fenichel, *Persistence and smoothness of invariant manifolds for flows*, Indiana Univ. Math. J., 21 (1971/1972), pp. 193–226.
[20] G. Froyland, S. Lloyd, and N. Santitissadeekorn, *Coherent sets for nonautonomous dynamical systems*, Phys. D, 239 (2010), pp. 1527–1541.
[21] G. Froyland and K. Padberg, *Almost-invariant sets and invariant manifolds—connecting probabilistic and geometric descriptions of coherent structures in flows*, Phys. D, 238 (2009), pp. 1507–1523.
[22] G. Froyland, K. Padberg, M. England, and A. Treguier, *Detection of coherent oceanic structures via transfer operators*, Phys. Rev. Lett., 98 (2007), 224503.
[23] G. Froyland, N. Santitissadeekorn, and A. Monahan, *Transport in time-dependent dynamical systems: Finite-time coherent sets*, Chaos, 20 (2010), 043116.
[24] E. Grenier, C. Jones, F. Rousset, and B. Sandstede, *Viscous perturbations of marginally stable Euler flow and finite-time Melnikov theory*, Nonlinearity, 18 (2005), pp. 465–483.
[25] J. Gruendler, *The existence of homoclinic orbits and the method of Melnikov for systems in R^n*, SIAM J. Math. Anal., 16 (1985), pp. 907–931.
[26] J. Guckenheimer and P. Holmes, *Nonlinear Oscillations, Dynamical Systems and Bifurcations of Vector Fields*, Springer, New York, 1983.
[27] G. Haller, *Lagrangian structures and the rate of strain in a partition of two-dimensional turbulence*, Phys. Fluids, 13 (2001), pp. 3365–3385.
[28] G. Haller, *Lagrangian coherent structures from approximate velocity data*, Phys. Fluids A, 14 (2002), pp. 1851–1861.
[29] G. Haller and A. Poje, *Finite time transport in aperiodic flows*, Phys. D, 119 (1998), pp. 352–380.
[30] G. Haller and G.-C. Yuan, *Lagrangian coherent structures and mixing in two-dimensional turbulence*, Phys. D, 147 (2000), pp. 352–370.
[31] M. Hirsch, C. Pugh, and M. Shub, *Invariant manifolds*, Bull. Amer. Math. Soc., 76 (1970), pp. 1015–1019.
[32] P. J. Holmes, *Averaging and chaotic motions in forced oscillations*, SIAM J. Appl. Math., 38 (1980), pp. 65–80.
[33] P. Holmes and D. Whitley, *On the attracting set for Duffing's equation*, Phys. D, 7 (1983), pp. 111–123.
[34] J. Jimenez-Madrid and A. Mancho, *Distinguished trajectories in time dependent vector fields*, Chaos, 19 (2009), 013111.
[35] B. Joseph and B. Legras, *Relation between kinematic boundaries, stirring and barriers for the Antarctic polar vortex*, J. Atmospheric Sci., 59 (2002), pp. 1198–1212.
[36] T.-Y. Koh and B. Legras, *Hyperbolic lines and the stratospheric polar vortex*, Chaos, 12 (2002), pp. 382–394.
[37] C. Lu, *On the existence of periodic solutions of a forced Duffing equation*, Dyn. Contin. Discrete Inpuls. Syst. Ser. B Appl. Algorithms, 10 (2003), pp. 88–91.
[38] N. Malhotra, I. Mezić, and S. Wiggins, *Patchiness: A new diagnostic for Lagrangian trajectory analysis in time-dependent fluid flows*, Internat. J. Bifur. Chaos Appl. Sci. Engrg., 8 (1998), pp. 1073–1094.
[39] A. Mancho, D. Small, S. Wiggins, and K. Ide, *Computation of stable and unstable manifolds of hyperbolic trajectories in two-dimensional, aperiodically time-dependent vector fields*, Phys. D, 182 (2003), pp. 188–222.

[40] V. K. Melnikov, *On the stability of the centre for time-periodic perturbations*, Trans. Moscow Math. Soc., 12 (1963), pp. 1–56.
[41] K. Meyer and G. Sell, *Melnikov transforms, Bernoulli bundles, and almost periodic perturbations*, Trans. Amer. Math. Soc., 314 (1989), pp. 63–105.
[42] I. Mezić and S. Wiggins, *A method for visualization of invariant sets of dynamical systems based on the ergodic partition*, Chaos, 9 (1999), pp. 213–218.
[43] P. Miller, C. Jones, A. Rogerson, and L. Pratt, *Quantifying transport in numerically generated velocity fields*, Phys. D, 110 (1997), pp. 105–122.
[44] K. Palmer, *Exponential dichotomies and transversal homoclinic points*, J. Differential Equations, 55 (1984), pp. 225–256.
[45] R. Pierrehumbert and H. Yang, *Global chaotic mixing in isentropic surfaces*, J. Atmospheric Sci., 50 (1993), pp. 2462–2480.
[46] A. Poje and G. Haller, *Geometry of cross-stream mixing in a double-gyre ocean model*, J. Phys. Oceanography, 29 (1999), pp. 1649–1665.
[47] A. Provenzale, *Transport by coherent barotropic vortices*, Ann. Rev. Fluid Mech., 31 (1999), pp. 55–93.
[48] V. Rom-Kedar, A. Leonard, and S. Wiggins, *An analytical study of transport, mixing and chaos in an unsteady vortical flow*, J. Fluid Mech., 214 (1990), pp. 347–394.
[49] R. Sacker and G. Sell, *The spectrum of an invariant submanifold*, J. Differential Equations, 38 (1980), pp. 135–160.
[50] B. Sandstede, S. Balasuriya, C. Jones, and P. Miller, *Melnikov theory for finite-time vector fields*, Nonlinearity, 13 (2000), pp. 1357–1377.
[51] J. Scheurle, *Chaotic solutions of systems with almost periodic forcing*, J. Appl. Math. Phys. (ZAMP), 37 (1986), pp. 12–26.
[52] S. Shadden, F. Lekien, and J. Marsden, *Definition and properties of Lagrangian coherent structures from finite-time Lyapunov exponents in two-dimensional aperiodic flows*, Phys. D, 212 (2005), pp. 271–304.
[53] R. Vinograd, *Exact bounds for exponential dichotomy roughness* I. *Strong dichotomy*, J. Differential Equations, 71 (1988), pp. 63–71.
[54] M. Wechselberger, *Extending Melnikov theory to invariant manifolds on non-compact domains*, Dyn. Syst., 17 (2002), pp. 215–233.
[55] L. Weiguo and S. Zuhe, *A constructive proof of existence and uniqueness of 2π-periodic solutions to Duffing's equation*, Nonlinear Anal., 42 (2000), pp. 1209–1220.
[56] S. Wiggins, *Chaos in the quasiperiodically forced Duffing oscillator*, Phys. Lett. A, 124 (1987), pp. 138–142.
[57] S. Wiggins, *Chaotic Transport in Dynamical Systems*, Springer-Verlag, New York, 1992.
[58] S. Wiggins, *Chaos in the dynamics generated by sequences of maps, with applications to chaotic advection in flows with aperiodic time dependence*, Z. Angew. Math. Phys., 50 (1999), pp. 585–616.
[59] K. Yagasaki, *The Melnikov theory for subharmonics and their bifurcations in forced oscillations*, SIAM J. Appl. Math., 56 (1996), pp. 1720–1765.
[60] K. Yagasaki, *The method of Melnikov for perturbations of multi-degree-of-freedom Hamiltonian systems*, Nonlinearity, 12 (1999), pp. 799–822.
[61] K. Yagasaki, *Melnikov's method and co-dimension two bifurcations in forced oscillations*, J. Differential Equations, 185 (2002), pp. 1–24.
[62] K. Yagasaki, *Invariant manifolds and control of hyperbolic trajectories on infinite- or finite-time intervals*, Dyn. Syst., 23 (2008), pp. 309–331.
[63] K. Yagasaki and T. Wagenknecht, *Detection of symmetric homoclinic orbits to saddle-centres in reversible systems*, Phys. D, 214 (2006), pp. 169–181.
[64] Y. Yi, *A generalized integral manifold theorem*, J. Differential Equations, 102 (1993), pp. 153–187.